12-2018

Electrochemical and morphological properties of chloride-doped lithium argyrodite solid electrolytes.

William Richard Arnold
University of Louisville

ELECTROCHEMICAL AND MORPHOLOGICAL PROPERTIES OF CHLORIDE-DOPED LITHIUM ARGYRODITE SOLID ELECTROLYTES

By

William Richard Arnold
B.S. University of Kentucky, 2016
M.S. University of Louisville, 2018

A Thesis Submitted to the Faculty of the J.B. Speed School of Engineering
of the University of Louisville
in Partial Fulfillment of the Requirements
for the Degree of

Master of Science
in Mechanical Engineering

Department of Mechanical Engineering
University of Louisville
Louisville, Kentucky

December 2018

ELECTROCHEMICAL AND MORPHOLOGICAL PROPERTIES OF CHLORIDE-DOPED LITHIUM ARGYRODITE SOLID ELECTROLYTES

By

William Richard Arnold
B.S. University of Kentucky, 2016
M.S. University of Louisville, 2018

A Thesis Approved on

December 13, 2018

by the following Thesis Committee:

_____

Dr. Hui Wang

_____

Dr. Peter Quesada

_____

Dr. Noppadon Sathitsuksanoh

DEDICATION

This thesis is dedicated to my parents, Anne and Bobby Arnold.

ACKNOWELDGEMENTS

First and foremost, I would like to acknowledge and thank my advisor and PI, Dr. Hui Wang, who guided me throughout every learning curve I've faced over the past year, as well as to Dr. Quesada and Dr. Tik for all their help and for sitting on my committee. I would like to acknowledge the Department of Mechanical Engineering and the Conn Center at UofL for all their assistance. I would also like to thank Dr. Dominika Ziolkowska, who was tasked with training a mechanical engineering student in the ways of chemistry. Also, thanks to Dr. Mahendra Sunkara, Dr. Kevin Murphy, Dr. Jacek Jasinski, and Rachel DeWees, who were so helpful and willing to teach me. Finally, I would like to acknowledge my brothers, Robert and Winston, for keeping me grounded and always being available for advice.

ABSTRACT

ELECTROCHEMICAL AND MORPHOLOGICAL PROPERTIES OF CHLORIDE-DOPED LITHIUM ARGYRODITE SOLID ELECTROLYTES

William R. Arnold

December 13, 2018

Recently, much attention has been devoted to the development of solid electrolytes to be used in all-solid-state-batteries. One group of promising solid electrolyte (SE) materials are lithium argyrodites, a class of superconductors which are noted for their high ionic conductivities. In particular, halogen doping has been shown to increase both conductivity and stability. The majority of research has focused on material synthesis through solid state reactions, but a novel liquid synthesis method for the preparation of Cl-doped Li_7PS_6 solid electrolyte provides the advantages of a homogenous product and a rapid, economic synthesis. Here this thesis focuses on the liquid synthesis process in two parts: (1) examine the effect of Cl content on the structure and conductivity of $Li_{5+x}PS_{6-x}Cl_x$ solid electrolytes ($1 \leq x \leq 3$); (2) investigate the effects of the reaction process parameters (mixing time, mechanical agitation, temperature) on the structure and conductive properties of Li_6PS_5Cl. The results show that $Li_7PS_4Cl_2$ (with 2 mols of chloride) achieved the highest ionic conductivity of $4.4 \times 10^{-4}\ S\ cm^{-1}$ at room temperature, as well as excellent stability with lithium metal up to 5 V. Beyond 2 mols of doped chloride the performance gets rapidly worse. The results also indicate that longer

mixing time up to 5 hours yields a higher conductivity of $5 \times 10^{-4}\ S\ cm^{-1}$, but does not obviously affect the phase purity and grain size. Mechanical agitation also does not appear to affect the phase or conductivity, however, a high sintering temperature results in a negative effect on the electrochemical performance. These results provide insight and understanding into this new liquid synthesis process which will play a huge factor in the future of solid-state-battery technology.

TABLE OF CONTENTS

LIST OF FIGURES

1.0 INTRODUCTION

Since their invention in 1991, lithium-ion batteries have been the battery-of-choice when providing power to small electronic devices. In many ways they are ideal for this task. Li-ion batteries are stable over many cycles, they are lightweight, highly energy dense, and rechargeable. For these reasons they have become standard in most portable devices, and have played a vital role in many of the technological revolutions of the past 30 years [Ma, 2018]. More recently, Li-ion batteries have been looked to for powering larger-scale applications. The technology has even found its way into space, as NASA makes extensive use of Li-ion batteries, although this usage is always accompanied by strict safety guidelines and extra insulating packing material [Walker, 2015]. Li-ion batteries are an attractive option for car manufacturers, but here too, safety issues have held back significant progress. Electric cars, cell phones, and NASA equipment all share the same problem, a problem which is intrinsic to every Li-ion battery currently on the market: Li-ion batteries are flammable.

This flammability stems from the conventional Li-ion battery structure (*Figure 1*). All batteries are composed of a positive cathode, a negative anode, and an electrolyte which acts as an interface between the two. These three parts can be comprised of many different materials which provide different batteries with a wide range of cycle lives, voltage outputs, chemical stabilities, etc. Li-ion batteries (so named because they make

use of lightweight lithium ions to initiate electrical flow) have likewise had many designs over the years, but perhaps the most common is represented by a $LiCoO_2$ cathode, a graphene anode, and an organic liquid electrolyte which separates the two. While the electrodes may vary, the electrolyte typically remains the same for all commercial Li-ion batteries. But for battery manufacturers today, it is the liquid electrolyte which is the primary concern, as it is this volatile substance which is responsible for all the safety issues traditionally associated with Li-ion batteries, and it can be pushed to its limit in several different ways.

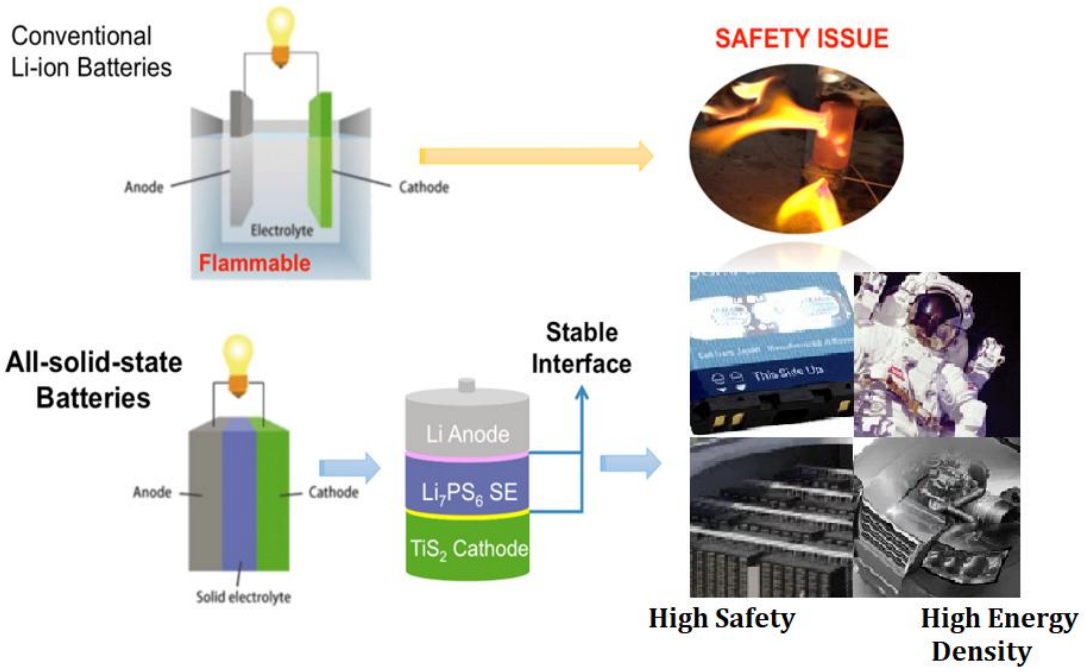

Figure 1. Conventional Li-ion batteries use a flammable organic liquid electrolyte which can lead to thermal runaway. The proposed all-solid-state battery would replace this with an inorganic solid material.

Overcharging, for example, can lead to the deposition of solid lithium within the electrolyte. Over time this solid lithium forms dendrites which can reach across the electrolyte and connect the electrodes, leading to a short. When shorted, a process known as thermal runaway can occur, whereby temperature increases exacerbate the performance of the battery and create a positive feedback loop that often leads to smoking and flames [Walker, 2015]. Solid lithium depositions within the electrolyte can also lead to the decomposition of the organic solvents, which are converted into harmful carbon monoxide and carbon dioxide. The expansion of these gases builds pressure and temperature within the battery that can lead to smoking and fire [McKissock, 2009]. More potential hazards include the common practice of using oxides to construct the cathode. Under high voltage, this oxygen can be released into the electrolyte which, in addition to increasing local pressure within the battery, creates an environment that is particularly prone to catching fire [McKissock, 2009]. Other types of stress, such as external mechanical, chemical, or thermal stresses, can also damage internal stability and lead to thermal runaway. These safety issues are some of the primary reasons electric car manufacturers are wary of roads filled with Li-ion battery-powered cars, or why NASA must add heavy insulating material for all their research involving batteries.

As such, there has been a push in recent years for the development of an all-solid-state battery. These batteries, which use solid ion-conductors to replace organic liquid electrolytes in conventional Li-ion batteries, provide a promising alternative for next-generation batteries given their inherent high safety and energy density [Ma, 2018; Zhang, 2018; Wang, 2016; Kim, 2017]. Solid electrolytes (SE) are made of inorganic material, and thus they lack the volatile organic solutes which can sublimate and increase

local pressure. It is possible for solid lithium to deposit within solid electrolytes, but this occurs at a slower rate than in their liquid counterparts, and it is much less likely that these dendrites will ever lead to a short [Ma, 2018]. Thermal runaway is often caused by the leaking and exposing of the liquid electrolyte to the atmosphere, another problem which does not exist when using solid electrolytes [Walker, 2015]. Applications such as electric vehicles, which might have presented serious safety issues with traditional Li-ion batteries, could be manufactured risk-free if all-solid-state batteries were used.

The reason that all-solid-state batteries have not yet been implemented on a large scale is simply because their performance still lags behind conventional liquid electrolytes. A suitable solid electrolyte would need to show a high ionic conductivity at least on the scale of 10^{-4} S cm^{-1}, a wide electrochemical window of at least 5 V, stability over many cycles, and a high energy density [Ma, 2018]. There are many possible options, like oxides (e.g. LLTO, LLZO, LMNO), or phosphates (e.g. LPON, LTAP), many of which are based off the Na superconductor NASICON structure [Bachman, 2016]. However a great deal of interest has been directed towards sulfide-based solid electrolytes, whose excellent conductivities (10^{-4} S cm^{-1}–10^{-3} S cm^{-1}), high thermal and electrochemical stability, good mechanical properties, and low impedance interface make it an attractive candidate for future use in all-solid-state batteries [Ma, 2018].

Even amongst sulfide-based solid electrolytes there are many possible options. One of the more promising options comes from the mineral family known as argyrodites [Deiseroth, 2008]. Argyrodites were first represented by Ag_8GeSe_6, which was amongst the early contenders for possible future solid electrolytes due to their high

intrinsic ionic conductivity (up to 10^{-2} S cm^{-1}). Ag_8GeSe_6 would be prohibitively expensive to produce at scale, however. Lithium argyrodites (e.g. Li_7PS_6), a class of sulfide-based Li-ion superconductors based on the general chemical structure observed in Ag_8GeSe_6, are synthesized by substituting Ag^+ atoms with Li^+, and the chalcogen Se^{2-} with S^{2-} [Deiseroth, 2008]. Synthesis of lithium argyrodites comes primarily from the creation of an Li_2S-P_2S_5 composite. A common, lower-order example is Li_3PS_4, which our lab was able to synthesize in an organic acetonitrile solvent [Ziolkowska, 2018]. Higher order argyrodites have also been reported, such as $Li_7P_3S_{11}$, which *Wang et al.* was able to create via a liquid synthesis, also in acetonitrile solvent [Wang, 2016]. Halide-doped lithium argyrodites Li_6PS_5X (X= Cl, Br, I) have also been synthesized, and have been reported to provide Li-ions with intrinsic mobility in the range of 10^{-3}–10^{-4} S cm^{-1} at room temperature, which is on par with their liquid counterparts [Rayavarapu, 2011; Rao, 2011; Yu, 2016]. Li_6PS_5X is made from the same Li_2S-P_2S_5 amalgamation, but LiX is also incorporated into the synthesis in a process known as doping. Across many different solid electrolyte materials, doping has been shown to improve electrochemical performance and enhance stability [Ma, 2018]. This holds true for sulfide solid electrolytes as well [Deiseroth, 2011]. Although Li_6PS_5X (X= Cl, Br, I) shows similar crystalline structures and diffraction patterns across all the halides, the choice of which halide to use does influence ion-transport and electrochemical properties. *Rao et al.* reported that the Li-ion nobilities in Li_6PS_5Cl and Li_6PS_5Br are higher than Li_6PS_5I because the larger I^{1-} cannot easily be exchanged for S^{2-} [Rao, 2011]. *Boulineau et al.* compared the different argyrodites and found that Li_6PS_5Cl shows no oxidation and reduction peaks up to 7.0 V vs. Li/Li^+ [Boulineau, 2012]. With such intrinsically high Li-

ion conductivity and stability, Li-argyrodites materials are amongst the most promising of all possible solid electrolyte candidates. Additionally, previous work has demonstrated that solid state batteries made with Li_6PS_5Cl or Li_6PS_5Br as the solid electrolyte (coupled with various possible cathode materials: S, Li_2S, and MoS_2, etc.) retain a high capacity and good cycling stability [Chida, 2018; Auvergniot, 2016; Yu, 2016; Yubuchi, 2015]. Both Li_6PS_5Cl and Li_6PS_5Br seem like suitable candidates, but in general Li_6PS_5Cl has been reported to have higher stability and slightly higher ionic conductivity. As such, Li_6PS_5Cl is the material of interest for this project. The primary purpose of this work is to investigate the effect that variations in the doping content would have on the performance of the solid electrolyte.

The three common methods used to prepare Li-argyrodites are: (1) mechanical alloying; (2) mechanical alloying followed by annealing; (3) solid-state sintering [Boulineau, 2012; Kraft, 2017; Auvergniot, 2017]. These methods are time intensive, often requiring extended ball milling of up to 72 hours followed by a long sintering time. The sintering itself is also an issue, as materials mixed exclusively through mechanical means require a rather high temperature to properly crystallize, sometimes as high as 550°C [Boulineau, 2018]. This energy-intensive process presents a problem for possible future applications. For solid state batteries to be scaled for industrial and commercial use, their synthesis needs to be fast and cheap. Recently, our lab has developed a two-part liquid synthesis technique which can greatly increase production time while also decreasing energy intensiveness. After first preparing Li_3PS_4 via an organic solvent and low (140°C) temperature, Li_7PS_6 lithium argyrodite can then be

prepared by mixing Li_3PS_4 with Li_2S in an inexpensive ethanol solvent. The mixing process takes only one hour, and the sintering only an hour more [Ziolkowska, 2018]. Given a maximum sintering temperature of 200°C and a total synthesis time of only 3 hours, Li_7PS_6 appears to be amongst the least energy intensive sulfide-based solid electrolyte materials which currently exists.

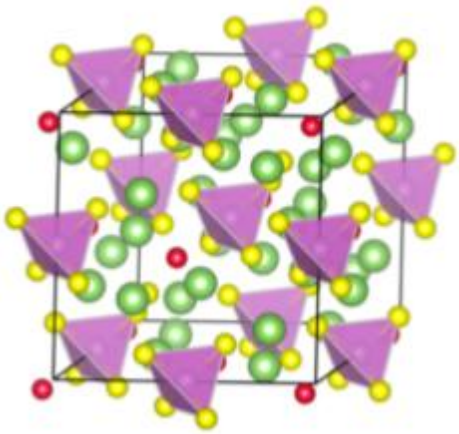

Figure 2. Structural model of Li_6PS_5Cl. Light green represents Li^+, red represents Cl^-, yellow represents S^{2-}, and purple represents $(PS_4)^{3-}$ tetrahedron [Ma, 2018].

Solid electrolytes are unique in that they allow for the migration of lithium ions through an inorganic matrix of crystallized grains that have been pressed into a small, thin pellet. This phenomenon is possible due to the unique characteristics that solid electrolyte materials display. Lithium has three main pathways as it makes its way through a solid lithium argyrodite (*figure 3*): (1) the first is a triplet jump whereby lithium moves between two vacant 48h sites via an intermediary 24g site, [2] the second pathway involves the formation of a "cage" structure whereby lithium can jump between different triplets, [3] and the third describes the pathways that are formed between the different

"cages" themselves [Rolson, 2016; Yu, 2016]. In practice, all three halide doped argyrodites contain the first two pathways — a fact which only services to move lithium ions back and forth within a single cage, never to actually make it through. The reason Cl-doped argyrodites perform the best of the three is because they contain a higher frequency of the third pathway. This allows for lithium ions to move freely throughout the entire solid, in addition to lowering grain boundary resistance [Rolson, 2016; Yu, 2016].

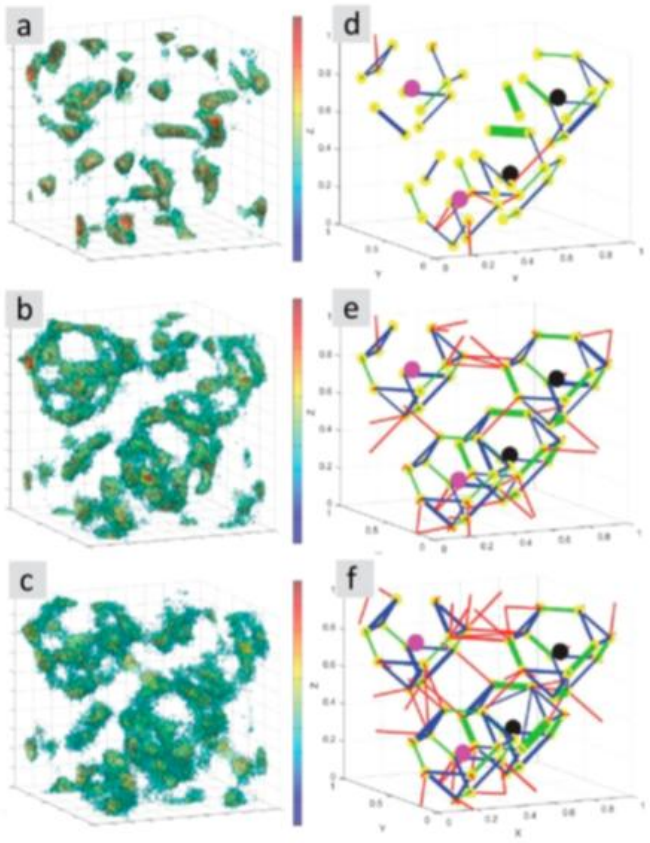

Figure 3. (a-c) An MD simulation representation of Li_6PS_5Cl heated to (a,d) 300 K, (b,e) 450 K, and (c,f) 600 K. (d-e) shows jump statistics representing three types of Li-ion migrations: (green) a triplet jump between two vacant 48h sites; (blue) migration between

the triplet jumps to form a "cage" structure; (red) migrations between the cages [Yu, 2016].

One possible way of increasing ionic conductivity involves controlling for the grain size of the synthesized materials. The relationship between the two is not always straightforward—depending on the material used smaller grain size can be either beneficial or detrimental to ionic conductivity, and it is currently impossible to determine this without experimental results [Wu, 2017]. There also appears to be a "sweet spot" with many materials, where a particular grain size provides the best results, and anything smaller or larger than that size negatively affects performance [Bi, 2017]. This relationship is dependent on the two types of ionic conductivity that are present in crystalline solid electrolytes. The first type—bulk ionic conductivity—refers to the flow of ions through the crystal itself. Bulk conductivity is typically more influential when grain size is larger. Conversely, grain boundary ionic conductivity refers to the flow of ions along the spaces in between the grains [Dawson, 2018].

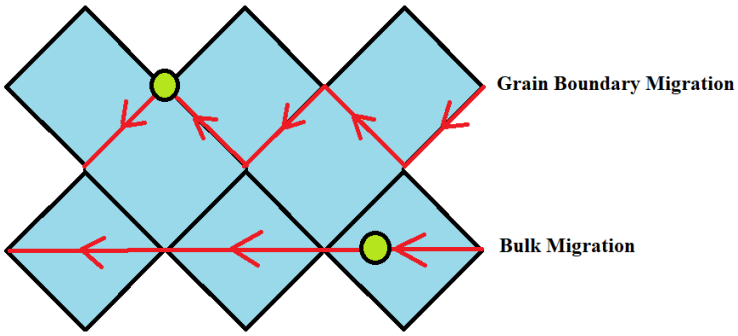

Figure 4. Individual Li ions travel either via the grain boundaries or through the bulk of the crystal itself. The lack of atomic vacancies at the grain boundaries usually inhibits ionic conductivity

As grain size decreases, the overall grain boundary surface area increases which increases the influence that grain boundary conductivity will have. In practice, both the bulk and grain boundary conductivity will influence the ionic flow for all grain sizes. The challenge then becomes finding the right balance between the two. That said, ionic conductivity is not the only performance variable related to grain size. Many papers have noted a relationship between the grain boundary and activation energy. However, this does appear to be a straightforward relationship, as grain boundary activation energy has been noted to consistently be larger than bulk activation energy [Dawson, 2018].

In general, there has been very little work done regarding the relationship between lithium-based solid electrolytes and grain size, and even less that has looked at this relationship with regards to lithium argyrodites. Of note is the wide variance in reported ionic conductivity (10^{-5} S cm^{-1}–10^{-3} S cm^{-1}) and activation energy (0.56 eV–0.11 eV) that exists in the literature [Yu, 2016]. This discrepancy can possibly be attributed to not controlling for a particular grain size during synthesis. *Dawson et. al* performed a MD simulation of the migration of lithium ions through the Li-based perovskite Li_3OCl. They report that within the bulk structure, Li-ions migrate due to vacancies in Li-sites along the three-tiered "cage" pathways [Dawson, 2018; Rolson, 2016; Yu, 2016]. This is not the case for grain boundary migration, as it was found that this movement was primarily due to the reduced atomic density at the grain boundaries themselves. This movement mechanism appears to be detrimental to ionic conductivity, as *Wu et. al* reports that it is the lack of Li-vacancies at the boundary which is responsible for poor grain boundary conductivity [Wu, 2017]. There is also an exchange between the two pathways, as Li-ions travelling via the grain boundaries can migrate into the bulk structure and vice-versa

[Dawson, 2018]. That said, they report that Li-ion migration within a polycrystalline material increases with increasing grain size. In fact, this is a trend that is seen across a wide array of possible solid electrolyte materials. This occurs due to the fact grain boundary resistance becomes less prominent as grain size increases. And it is this grain-boundary resistance which seems to be the dominant limiting factor at play in lithium-based solid electrolytes, and can contribute to a bottleneck effect if its effect is too pronounced. According to *Dawson et al.*, bulk conductivity starts having a more prominent effect on Li-ion movement through lithium perovskites when the grain size is roughly 400 nm, while anything below 100 nm results in conductivity dominated by grain boundaries [Dawson, 2018]. It is assumed then that this trend will continue for other Li-based solid electrolytes, and thus it stands to reason that controlling for larger grain sizes should yield better results.

Controlling for grain size can be a difficult endeavor, however, There are several schools of thought concerning the methodology. With regards to most synthesized solid electrolytes, temperature is the primary means of controlling for grain size [Sharafi, 2017; Huo, 2016; Wu, 2017; Huber, 2018; Bi 2017]. In general, higher temperatures and longer time periods are favorable to forming larger crystals. Our lab has previously experimented with higher temperatures, and has found that, unlike many others, our synthesized samples show a marked decrease in ionic conductivity when heated to above 200°C [Ziolkowska, 2018]. There are two possible explanations for why this is. Unlike other researchers, our lab employs a liquid synthesis which necessitates the use of a solvent. This solvent is evaporated away before sintering, but may still remain in large enough quantities to be affected by higher temperature. Additionally, our materials are

sintered under a vacuum pump. This pump creates an inert atmosphere for the material to crystallize, but it may also suck away loose sulfur ions, thus changing the material's characterization. If temperature is not a suitable agent for controlling grain size, then it is possible that this can be achieved by controlling the material integration: mixing time and stir rate. One of the primary goals of this work is to investigate the effect that control of process parameters—namely, mixing time, mechanical agitation, and temperature—would have on both the grain size and electrochemical properties of the solid electrolytes.

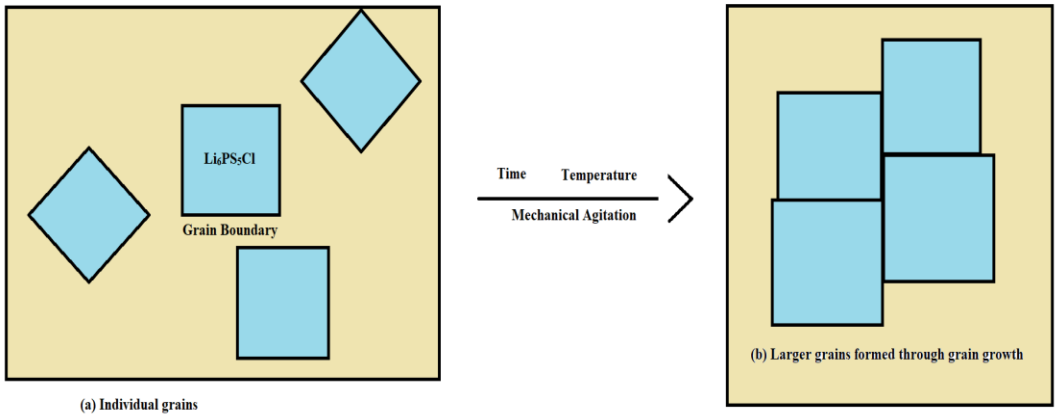

Figure 5. Grain growth typically occurs through application of longer synthesis times, higher temperatures, or control of mechanical agitation

2.0 METHODS AND MATERIALS

2.1 SYNTHESIS OF LI_3PS_4

Li_7PS_6 and $Li_{5+x}PS_{6-x}Cl_x$ were prepared in two steps, both of which employ a novel liquid synthesis technique. In order to synthesize an Li_7PS_6 lithium argyrodite or any of its halide-doped derivatives, an Li_3PS_4 precursor must first be synthesized. Li_2S is air sensitive (as are all the synthesized lithium argyrodites) and will quickly oxidize if exposed to regular atmosphere. As such, all preparation work for this experiment was done in a glove box under an inert argon atmosphere (*figure 6*). Li_3PS_4 was prepared by using the previously reported method of dissolving Li_2S and P_2S_5 in a solvent, in our case tetrahydrofuran (THF) [Wang 2016]. The materials are mixed in a 3:1 ratio (Li_2S:P_2S_5) and left to stir in 40mL THF (yields ~2g materials) for ~12 hours in an argon atmosphere at room temperature before being double-filtered, leaving an isolated white powder. The powder was transferred to a glass oven tube and dried at 80°C under a vacuum (to evaporate the solvent) before being annealed at 140°C for 1 hour to form β-Li_3PS_4. The powder is then ground using a mortar and pestle for roughly 5 minutes before it is finished.

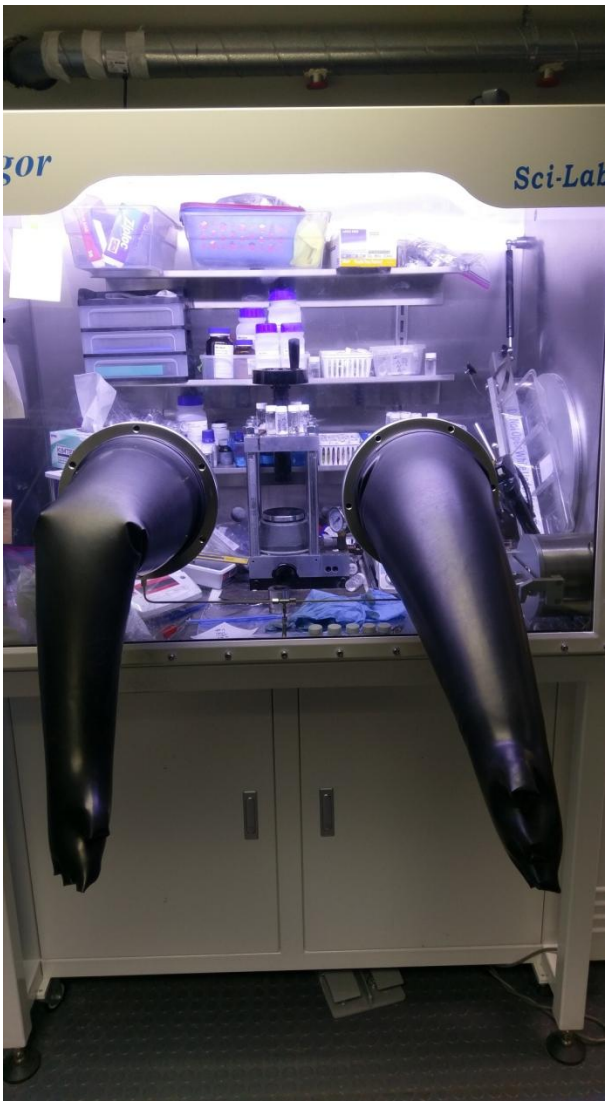

Figure 6. The primary glovebox used for materials preparation. It is filled with inert argon gas, and controls oxygen and water levels to under 1 ppm. The hydraulic press inside was used to densify solid electrolyte powder into thin pellets.

2.2 SYNTHESIS OF $LI_{5+X}PS_{6-X}CL_X$

Utilizing a method recently discovered in our lab, $Li_{5+x}PS_{6-x}Cl_x$ was synthesized by dissolving Li_3PS_4, Li_2S, and LiCl in ethanol in an argon atmosphere. Different stoichiometric ratios were used in order to determine which yielded the best results. For different combinations of Li_3PS_4:Li_2S:LiCl, we tested ratios of 1:2:0 (Li_7PS_6), 1:1:1 (Li_6PS_5Cl), 1:1:1.5 ($Li6.5PS_{4.5}Cl_{1.5}$), 1:1:2 ($Li_7PS_4Cl_2$), 1:1:2.5 ($Li_{7.5}PS_{3.5}Cl_{2.5}$), and 1:1:3 ($Li_8PS_3Cl_3$). First, Li_2S and LiCl are dissolved in ethanol (to help dissolve the LiCl, as Li_2S is easily soluble in ethanol), before Li_3PS_4 is added into the solution to be stirred. Following this, the solution is heated at 90°C under a vacuum until the ethanol has evaporated (usually not longer than 1 hour) before being annealed at 200°C for 1 hour. Again, the collected powder is ground using a mortar and pestle for 5 minutes.

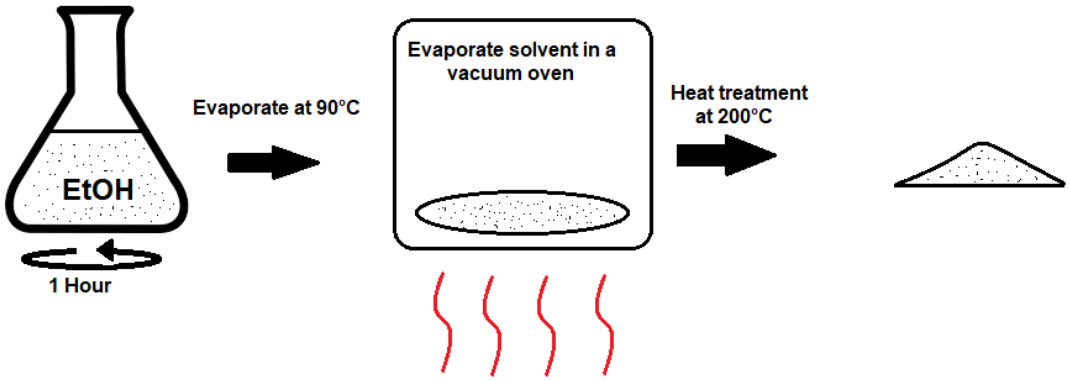

Figure 7. A schematic illustrating the basic process of synthesizing lithium argyrodite solid electrolytes

2.3 MATERIALS CHARACTERIZATION

The material was characterized by two methods: X-Ray Diffraction (XRD) and Raman spectroscopy. XRD is a technique which fires incident X-rays at a material sample and measures the photon's diffraction angles and intensities in order to determine what material it is. The 3-dimensional image which is captured can be displayed as angles on a 2-dimensional graph, which can then be filtered through a database in order to determine the sample material's chemical structure. Much work has been done on Li_6PS_5Cl in recent years, so it is easy to determine whether a pure sample has been synthesized. The literature indicates that Li_6PS_5Cl, as well as the pure phase Li_7PS_6, have strong XRD diffraction peaks at 2θ=25.3, 29.9, and 31.3°. XRD was performed using a Bruker D8 Discover (*figure 8*) with nickel-filtered Cu-Kα radiation (λ=1.5418 Å).

Figure 8. D8 Bruker Discover machine used for XRD characterization. For Li_6PS_5Cl, strong peaks are anticipated at 2θ=25.3, 29.9, and 31.3°.

Raman spectroscopy was also used to determine characterization. This method involves the firing of a laser at a material sample and measuring the molecular vibrations across different ranges of the electromagnetic spectrum. Due to these molecular excitations, the laser is shifted, which gives information about the molecular composition and shape of the sample material. Raman samples from the literature indicate the presence of vibrational modes attributable to local structural unit of PS_4^{3-}tetrahedral (421 cm^{-1}, 575 cm^{-1}), which is the primary vibrational mode associated with Li_6PS_5Cl. The Raman spectroscopy was measured using a Renishaw in Via Raman/PL Microscope and a 632.8 nm emission line of a HeNE laser.

Additionally, general morphologies of the samples were found using a TESCAN Vega3 scanning electron microscope (SEM). SEM allows for images of a sample material to captured at the μm scale. This will allow for different stoichiometric ratios of samples to be compared to determine if any visual differences are discernible between them.

2.4 ELECTROCHEMISTRY, AND CONDUCTIVITY

In order to perform ionic conductivity measurements, electrochemical impedance spectroscopy (EIS) was performed. This test uses a Bio-Logic SP200 to apply a voltage and measure the resultant impedance over a range of frequencies (5 MHz–1 Hz). To perform the measurements, 100 mg of the synthesized materials are pressed between carbon-coated aluminum (serving as blocking electrodes) into dense pellets under high pressure of 360 MPa to a disk roughly 1.27 cm (0.5") in diameter and 0.5 mm thick (*figure 9*). All preparations take place under an argon atmosphere. The pellets are tested

via either a swqgelok cell or a pressed cell using electrochemical impedance spectroscopy (EIS), and can be analyzed via a Nyquist plot. The impedance spectra forms a semi-circle at higher frequencies, which ends abruptly and is intercepted by a straight line (representing Li-diffusion from the blocking electrode) as lower frequency measurements are made. Impedance (or resistance) is determined via three maxima: The beginning of the semi-circle represents bulk impedance, the space between the start and end of the semi-circle represents the grain boundary impedance, and the sum of the two represents the total impedance (*figure 10*). The ionic conductivity is then derived from a relationship between the total resistance and the material's shape and size (*equation 2*).

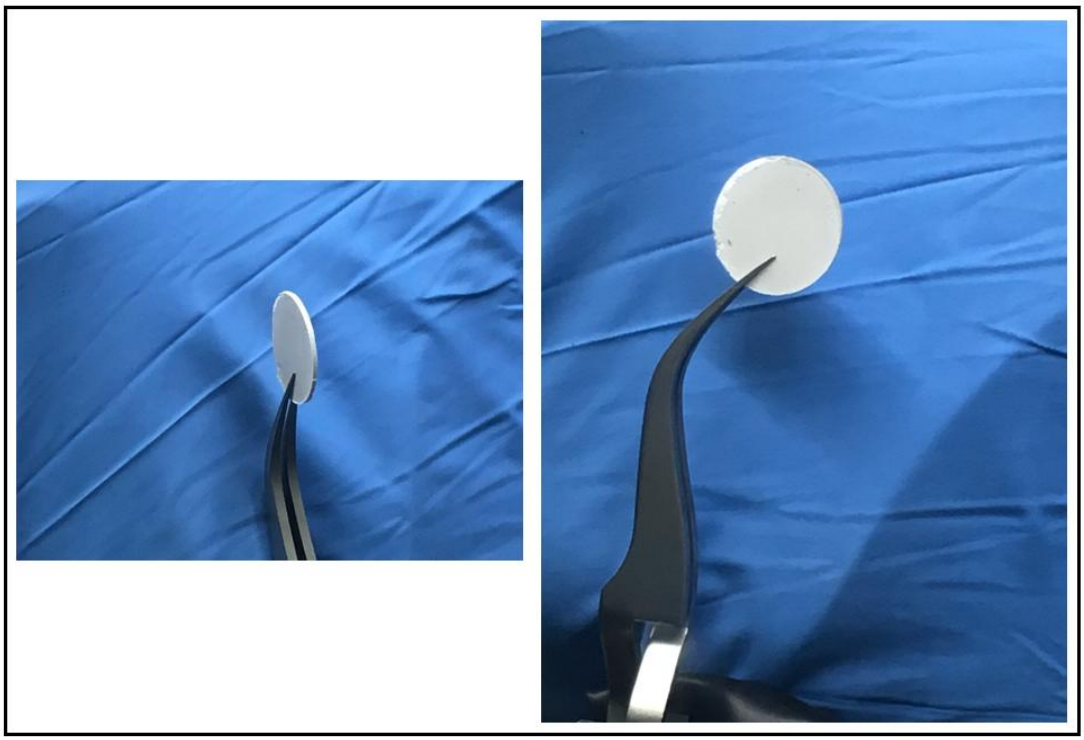

Figure 9. Solid electrolyte powder is pressed under 360 MPa to form a small pellet roughly 1.27 cm in diameter and 0.5 mm thick. Electrodes can be placed on either side to form a battery or to test electrochemical properties.

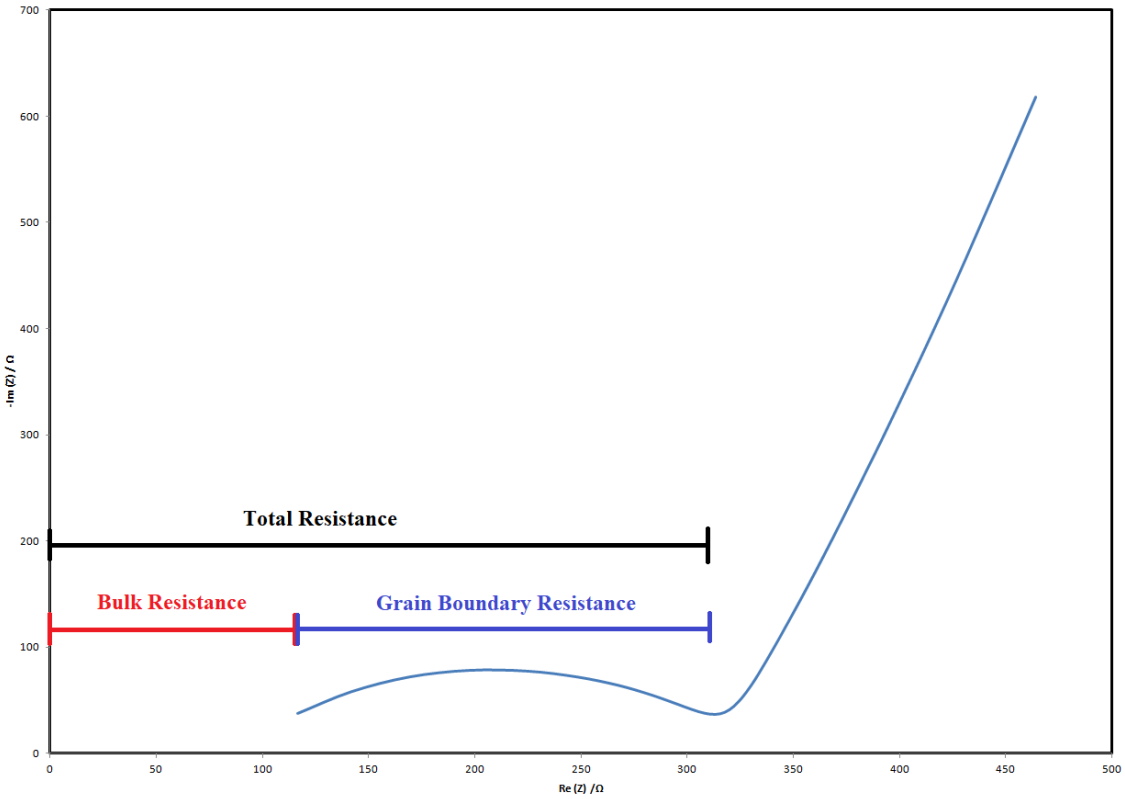

Figure 10. A Nyquist plot for a lithium argyrodite solid electrolyte. The resistance is determined from the semi-circle, and can be broken up into bulk and grain boundary resistances.

Equation 1. Ionic conductivity (**σ**) is determined from a relationship between the pellet's resistance (R), its area (A), and its thickness (L).

$$\sigma = \frac{A}{R \cdot L}$$

Additionally, impedance measurements can be used to produce Arrhenius plots, which come from temperature dependent spectra recorded from room temperature to 90°C. The data is logarithmic in nature, and is compared to an inverse temperature measurement to generate Arrhenius plots. Activation energy can be determined from the Arrhenius equation (*equation 2*).

Equation 2. The Arrhenius equation. (E_a) is the activation energy, (k) is the rate constant, (T) is the temperature, (R) is the gas constant, and (A) is a constant related to the geometry of the material.

$$k = Ae^{-E_a/RT}$$

2.5 ELECTROCHEMICAL STABILITY

The electrochemical stability of the synthesized materials was determined by both cyclic voltammetry and symmetric cell testing. Cyclic voltammetry tests are run in a Swagelok cell with a working electrode of solid lithium and a reference electrode of platinum (Li/SE/Pt cells) (*figure 11*). The working electrode's potential is quickly cycled between two preset voltages vs. Li/Li^+ and plotted against the resultant current. This method is useful for determining the short-term stability against high potentials.

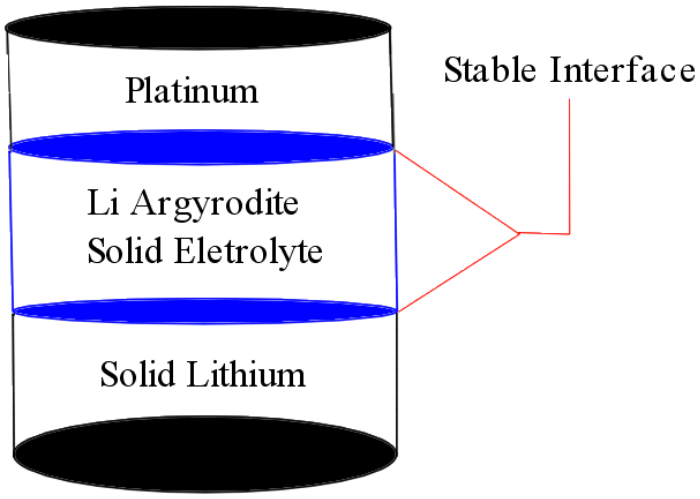

Figure 11. Cell setup used to test cyclic voltammetry properties of Li argyrodite solid electrolytes. A scaling voltage from -0.5–5 V is applied over several cycles and plotted against the resultant current.

Symmetric cell tests are constructed as Li/SE/Li cells, with solid lithium acting as electrodes on both sides (*figure 12*). A current density of 0.02–0.1 mA cm^{-2} was applied to the cell, and the resultant voltage is plotted verse time. This test is useful for determining the long-term stability of the materials, and is cycled for 72+ hours. Good performance indicates the presence of a strong electrode/electrolyte interface, which is one of the key challenges solid electrolytes face when implemented in full batteries.

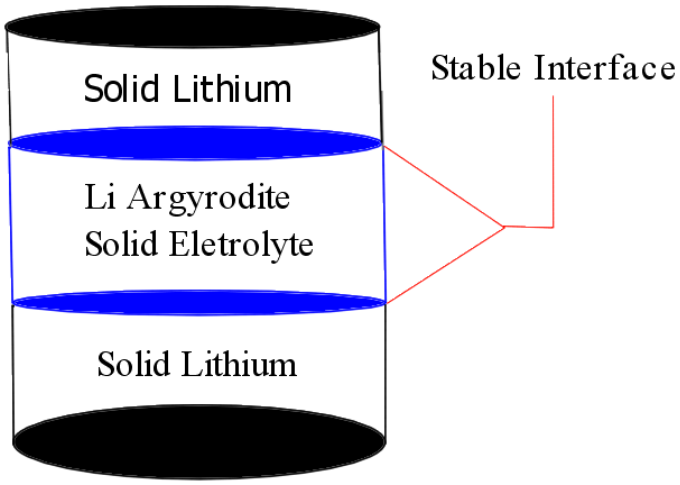

Figure 12. Cell setup used to test symmetric cell properties of Li argyrodite solid electrolyte. A current density from 0.02–0.1 mA cm^{-2} is applied and the resultant voltage is plotted against time. Stable interfaces are formed over long-term cycling.

2.6 CONTROL OF PROCESS PARAMETERS

Three process parameters were controlled for in an attempt to yield larger grain size: temperature, time, and mechanical agitation. Else wise, all experiments were run with the requisite materials to make Li_6PS_5Cl. Past results have indicated that the synthesized lithium argyrodites need to reach at least 200°C in order to properly crystallize. In order to determine the effect that temperature has on grain size and ionic conductivity, two samples were made and annealed at 250°C and 290°C, respectively.

A syringe pump was employed in order to control for synthesis mixing time. First, Li_2S and LiCl are dissolved in an ethanol solvent. This solution is put into a syringe pump and slowly pumped into dry Li_3PS_4. Some samples were prepared using a stir bar

for mechanical agitation. If so, the stir bar was turned on once enough ethanol was in the solution (*Table 1*). Else, the mixture was left to sit or was put straight into a heat treatment. XRD was performed on all the samples and an estimation of the grain size was found via the Scherrer Equation (*Equation 3*) program of DiffracEVA4.0 software. The Scherrer Equation uses the Full Width Half Maximum (FWHM) average of the XRD diffraction peaks, which themselves are dependent on the crystal size of the sampled material. Ionic conductivity and Arrhenius plots were also found via EIS tests.

Equation 3.

The Scherrer Equation, where (τ) is the mean crystal size, (β) is the FWHM, (K) is a shape factor, (λ) is the wavelength, and (θ) is the Bragg angle

$$\tau = \frac{K\lambda}{\beta \cos\theta}$$

Table 1.

Grain Size-Controlled Samples Grouped According to Pump Time, Stir Time, and Dissolution Time

*Sample was left to dissolve (without stirring) for 2.5 hours after pumping

Grain Size Sample	Pump Time	Stir Time
a	1 min	1 h
b	0.5 h	1 h
c	1 h	1 h
d	3 h	1 h
e	5 h	1 h
f*	1 h	0
g	5 h	0
h	1 h	0
i	0	0
j	0.5	0

3.0 RESULTS AND DISCUSSIONS

In summary, this project examined two different groups of lithium argyrodites. First were the argyrodites which were synthesized using different stoichiometric ratios of doped LiCl. These include Li_6PS_5Cl, $Li_{6.5}PS_{4.5}Cl_{1.5}$, $Li_7PS_4Cl_2$, $Li_{7.5}PS_{3.5}Cl_{2.5}$, and $Li_8PS_3Cl_3$, in addition to the pure phase Li_7PS_6. Also examined were the grain size-controlled samples, which include those found in *Table 1*, in addition to two samples which were heated to 250 and 290°C, respectively.

3.1 STRUCTURAL ANALYSIS OF Cl-DOPED LITHIUM ARGYRODITE

The solid electrolytes were characterized by X-ray diffraction (XRD). The XRD patterns for the powders for the chloride doped powders (*figure 13*) display sharp peaks at 2θ=25.3, 29.9, and 31.3°, corresponding to (220), (311), and (222) planes, respectively. These results match the diffraction patterns of past Li_6PS_5Cl material synthesized both through chemical means [Yubuchi, 2015] and mechanical means [Rao, 2013]. The XRD patterns for the pure phase Li_7PS_6 (space group F-43m) is very similar to its chloride doped counterpart, however it lacks peaks at 2θ=59.3 and 62.4°. The similarity between the two suggests the formation of a solid solution of Li_7PS_6 and LiCl. The XRD patterns reveal that crystallized Li_6PS_5Cl is the dominant phase of all the Cl-doped powders, although peaks corresponding to LiCl (2θ=34.9, 49.9°) begin to appear with the addition of excess LiCl. These peaks only appear with the addition of excess lithium chloride, indicating the purity of all the $Li_{5+x}PS_{6-x}Cl_x$ phases where $x \leq 1.5$. As

anticipated, the peaks corresponding to LiCl become slightly stronger with the addition of excess chloride. In the samples where x≥2, the presence of pure LiCl in the final solid solution indicates that this excess LiCl will not properly enter the Li_7PS_6 structure.

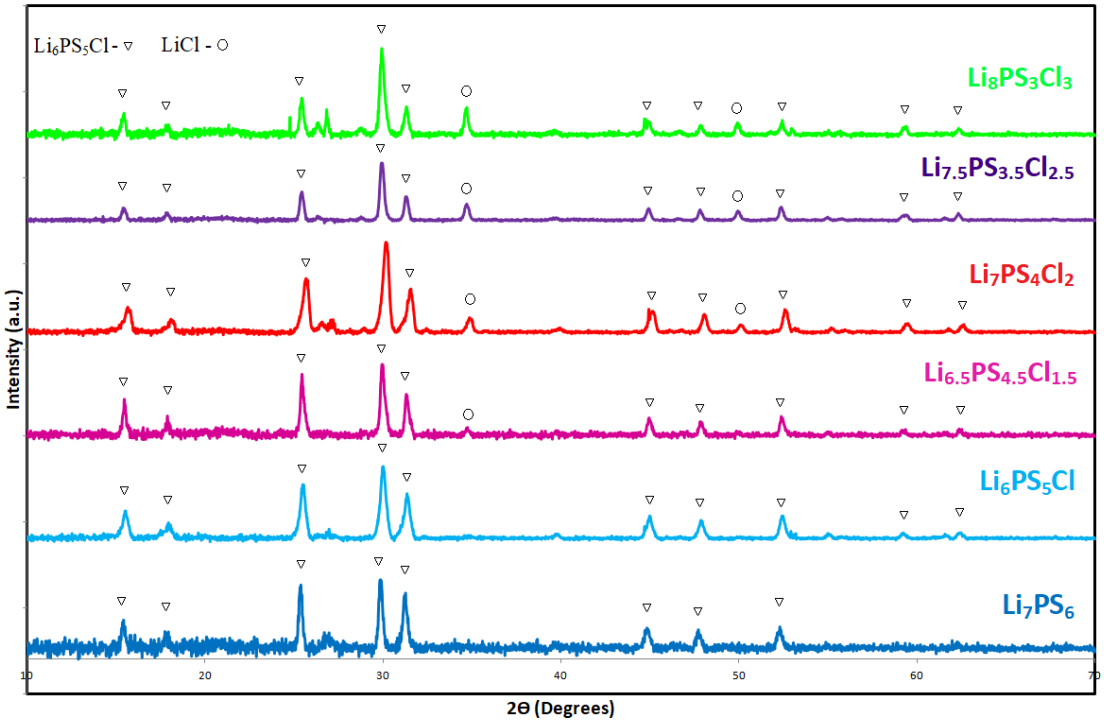

Figure 13. XRD diffraction patterns for the different stoichiometric ratios of prepared $Li_{5+x}PS_{6-x}Cl_x$ argyrodites. LiCl is present when x≥2.

Figure 14 shows the Raman spectra of the pure phase Li_7PS_6 and $Li_{5+x}PS_{6-x}Cl_x$ (1≤x≤3). All of the synthesized samples show a dominant peak at 421 cm^{-1}, which is attributable to the symmetric stretching mode of the P-S bond in PS_4^{3-}tetrahedra. This is also primary vibrational mode for argyrodite-type solid electrolytes [Yubuchi, 2015; Ziolkowska, 2018]. Additionally, a small peak at 575 cm^{-1} is observable in the chloride doped samples, which can be attributed to the asymmetric PS_4^{3-} vibrational mode. The excess addition of LiCl does not seem to influence the Raman spectra, however.

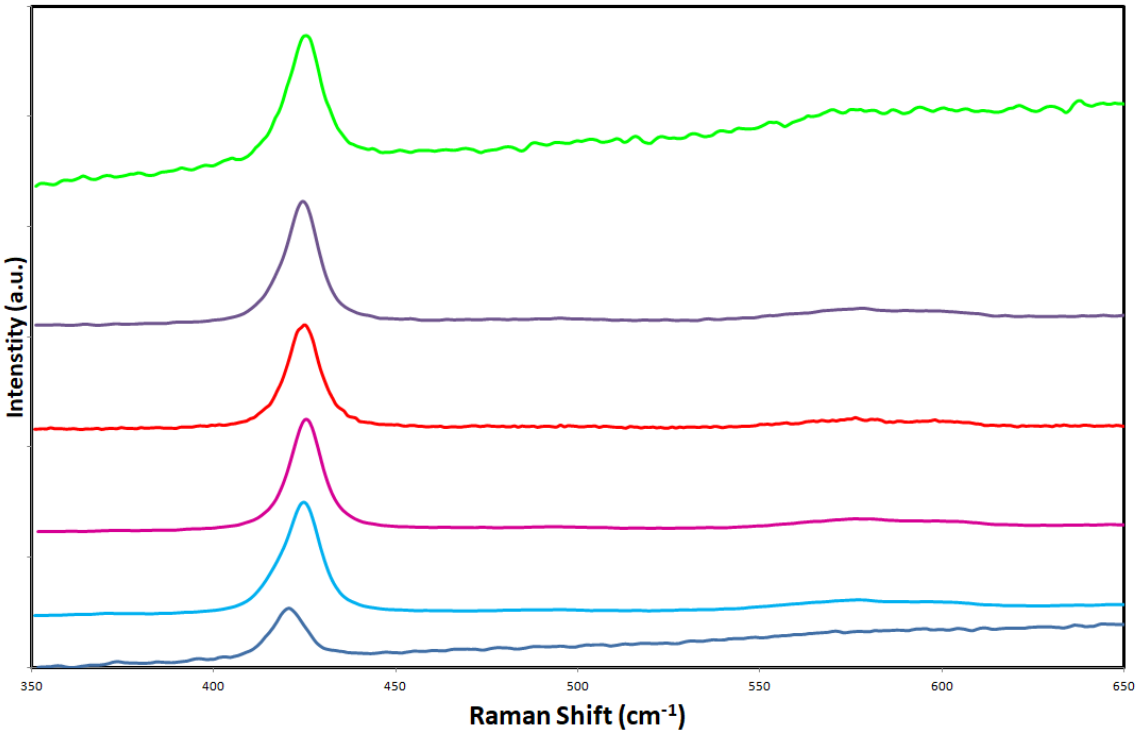

Figure 14. Raman shift of the different lithium argyrodites, grouped from bottom (Li_7PS_6) to top in ascending mols of LiCl. Vibrational modes are present at 421 cm^{-1}.

Scanning electron microscope was employed in order to capture a visual image of the different samples (*Figure 15*). At the 50 μm scale, no discernible difference can be made between any of the stoichiometrically different Cl-doped samples.

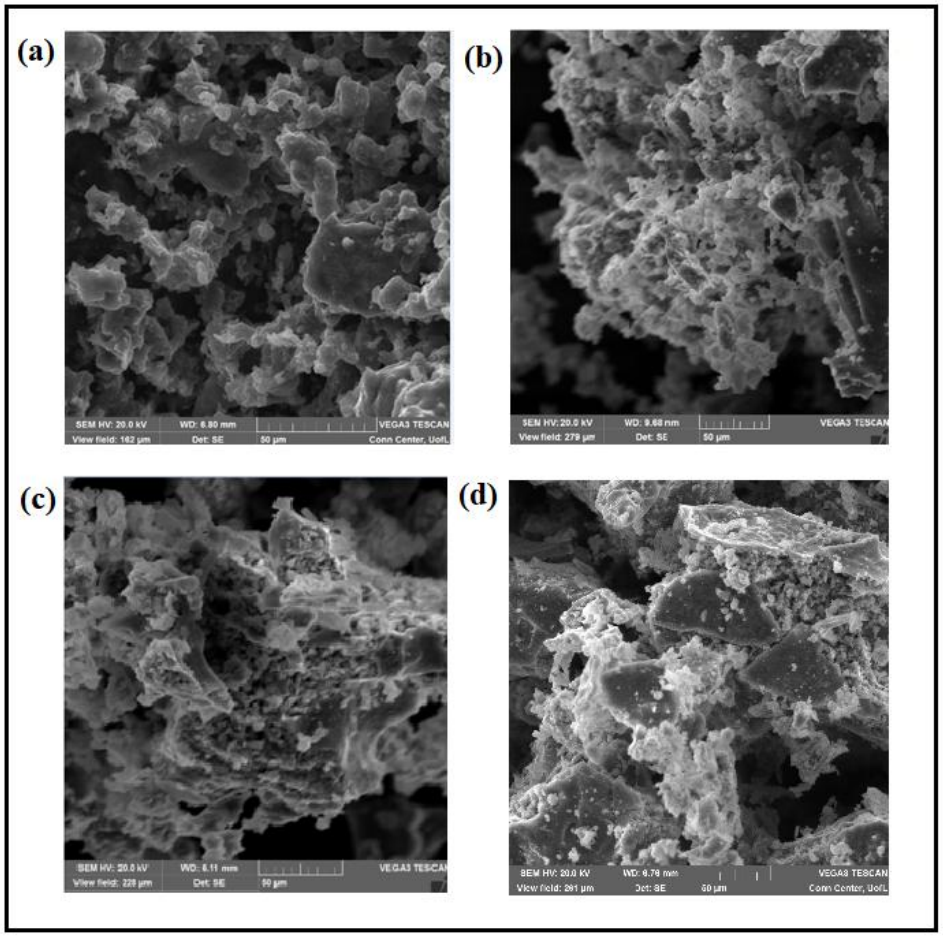

Figure 15. SEM images of (a) pure phase Li_7PS_6, (b) Li_6PS_5Cl, (c) $Li_7PS_4Cl_2$, and (d) $Li_8PS_3Cl_3$ at a scale of 50 μm.

3.2 ELECTROCHEMICAL ANALYSIS OF Cl-DOPED LITHIUM ARGYRODITE

The Li-ion conductivities of $Li_{5+x}PS_{6-x}Cl_x$ samples with different Cl doping contents were evaluated by electrochemical impedance spectra (EIS) measurements. The powder samples were cold-pressed under 360 MPa with Al/C foils as the blocking electrodes. The pure phase argyrodite Li_7PS_6 was tested and found to have an ionic conductivity of $1.9\times 10^{-5}\ S\ cm^{-1}$, while its Cl-doped counterpart Li_6PS_5Cl has an ionic conductivity of $2\times 10^{-4}\ S\ cm^{-1}$, more than 10 times higher (*figure 16*).

This positive effect continues when more doped chloride is added to the materials. Ionic conductivity continues to rise with $Li_{6.5}PS_{4.5}Cl_{1.5}$, and reaches its maximum value of $4.5\times 10^{-4}\ S\ cm^{-1}$ for $Li_7PS_4Cl_2$, which is the highest value yet to be achieved for lithium argyrodites prepared via liquid approaches [Ziolkowska, 2018]. The improved performance of the chloride doped argyrodites is due to the presence of LiCl in the EtOH solution, which replaces the sulfide atoms that normally occupy anion sites in the argyrodite's crystal structure [Rolson, 2016]. There are two explanations for why this atom replacement is beneficial. First is the space charging effect, which occurs due to differing charges between sulfide (S^{2-}) and chloride (Cl^{-1}) anions. The less electrochemically active chloride ions can only bond with one lithium ion at a time, as opposed to sulfide ions which can bond with two. This, in theory, would allow for more free lithium ions to make their way through the crystal structure when more chloride is present [Bachman, 2016]. Secondly, the crystallographic effect occurs because the halide ions occupy an entirely separate crystallographic position than sulfide ions. This causes the halide's interactions with flowing Li^+ ions to be decreased even further [Deiseroth, 2008]. When more mols of LiCl are added to the synthesis materials, this effect is heightened. In the case of $Li_7PS_5Cl_2$, all the anion sites are occupied by chloride. The presence of the chlorine halide affects which pathways the lithium ions will travel down, pressuring them towards the third, "cage"-connecting pathway [Rolson, 2016]. Because this pathway is most important for lithium conduction through the entire solid, it stands to reason that adding more halide will improve the conductivity, as has been displayed. However, when an excess of more than 2 mols of chloride are added to the mixture, the performance gets rapidly worse. XRD patterns show that pure LiCl is strongly present in

$Li_{x+5}PS_{6-x}Cl_x$ when $x \geq 2.5$. The poor performance of these samples can be attributed to the poor conductivity that LiCl displays on its own.

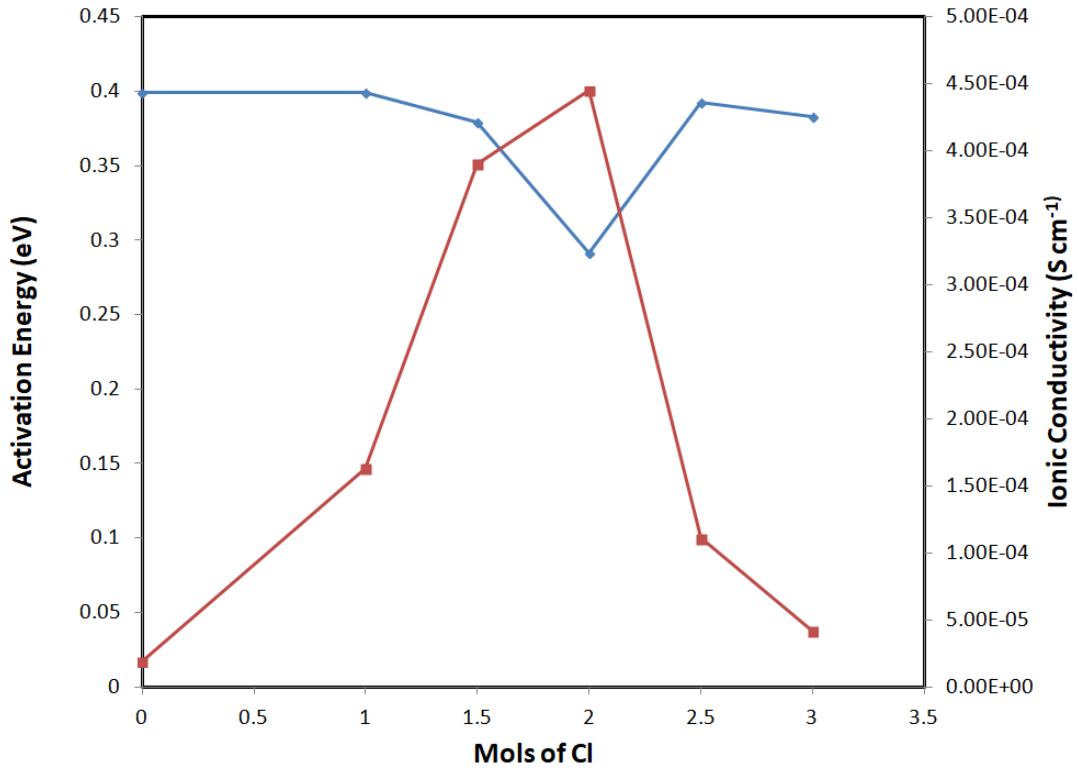

Figure 16. A comparison of the ionic conductivity and activation energy as a function of the number of mols of doped Cl present in the final product. A high conductivity of over $4.5 \times 10^{-4}\ S\ cm^{-1}$ is achieved when 2 mols of Cl are present.

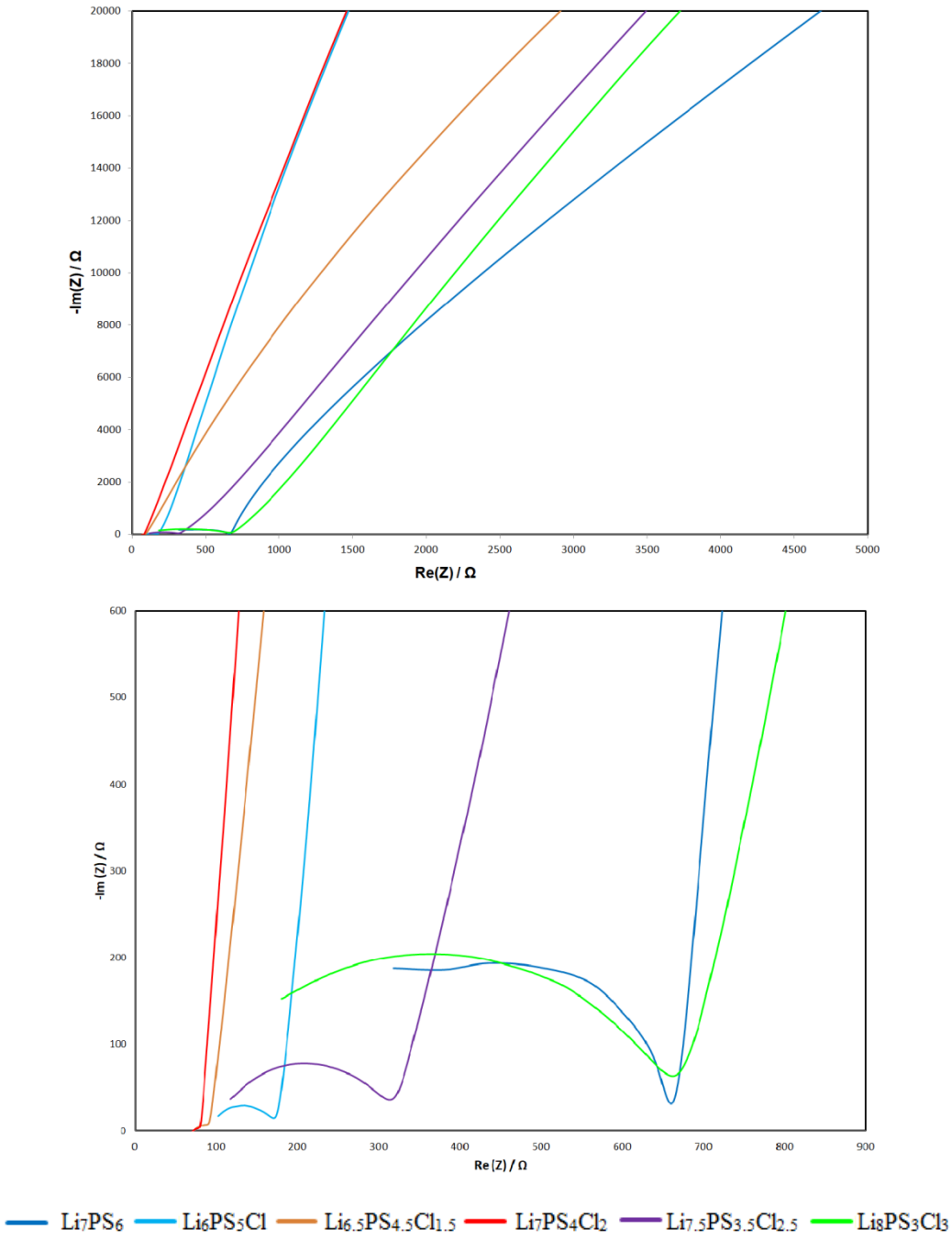

Figure 17. Nyquist plots from measured EIS tests. The lowest impedances are present when the argyrodite is doped with 2 mols of chloride.

Additionally, temperature dependent EIS tests were run in order to obtain Arrhenius plots for the different samples (*figure 18*). Ionic conductivities were determined from room temperature to 90°C for all samples, and plotted in order to determine activation energy (*figure 16*). The activation energy reflects the fluctuation of the ionic conductivity as temperature increases, and a smaller value reflects a better performing electrolyte. These tests indicate that, in addition to the highest ionic conductivity, $Li_7PS_4Cl_2$ also has the lowest activation energy of all the samples at 0.25 eV, which is one of the lowest values yet reported for halogen doped argyrodites [Boulineau, 2013; Rao, 2013]. $Li_7PS_4Cl_2$ was also able to achieve the highest ionic conductivity at increased temperature, reaching 3.5 mS cm^{-1} at 90°C. This in contrast to the excessively doped $Li_8PS_3Cl_3$, which was only able to reach a lower conductivity of 0.9 mS cm^{-1} at the same temperature.

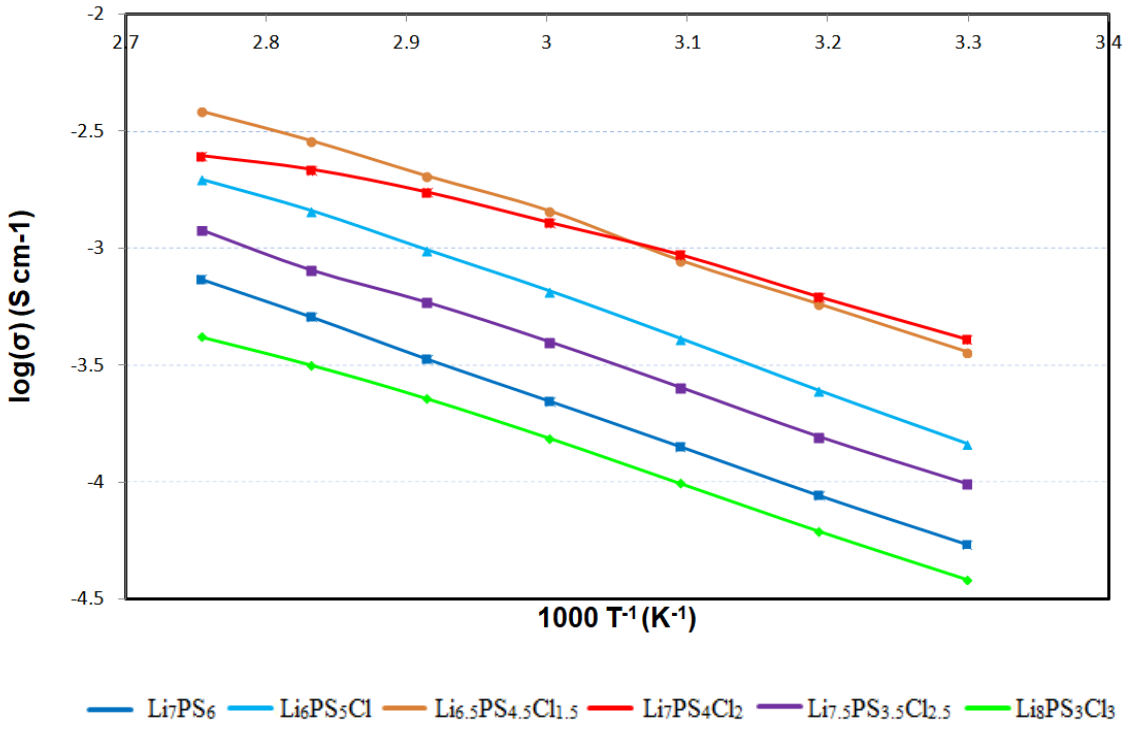

Figure 18. Arrhenius plots from EIS data, measured from room temperature to 90°C

In order to determine the electrochemical stability of the SEs, cyclic voltammetry was employed (*figure 19*). A cell consisting of $Li/Li_{x+5}PS_{6-X}Cl_x/Pt$ was constructed in a Swagelok cell, with solid lithium metal serving as the reference electrode and platinum acting as the working electrode. The different solid electrolytes were tested over a range of -0.5 V to 5.0 V (vs. Li/Li^+), with reversible oxidation and reduction peaks occurring around 0 V corresponding to anodic and cathodic deposition and dissolution, respectively. All synthesized electrolytes showed good stability over five cycles, which is ideal for battery use [Boulineau, 2012]. Additionally, no side reactions are observed up to 5 V for any of the samples, indicating they are all stable with metallic lithium. This is important, as solid lithium is known for its highly electrochemically reactive nature, and would serve as an excellent electrode. But due to its tendency to form lithium dendrites in liquid electrolytes, it has not been implemented on a large scale. These results indicate that all-solid-state batteries utilizing lithium argyrodites may readily be made with solid lithium metal as an electrode. $Li_7PS_4Cl_2$ performed the best in cyclic voltammetry as well, achieving strong anodic and cathodic currents of 40 and -50 mA, respectively.

Symmetric cell tests (*figure 20*) were run in order to determine the long-term cyclability and stability of metallic Li with $Li_{x+5}PS_{6-x}Cl_x$ solid electrolyte. The symmetric cell consisting of $Li/Li_{x+5}PS_5Cl_x/Li$ was constructed in a swagelok cell and was subject to current densities of 0.02–0.05 mA cm^{-2} at room temperature. The resulting voltage remained constant, indicating a stable interface and a small interfacial resistance between $Li_{5+x}PS_{6-x}Cl_x$ and Li. The cells were cycled over 72 hours at several different currents, after which shining lithium was able to be peeled away from the solid electrolyte. This indicates good cyclability over a long period of time.

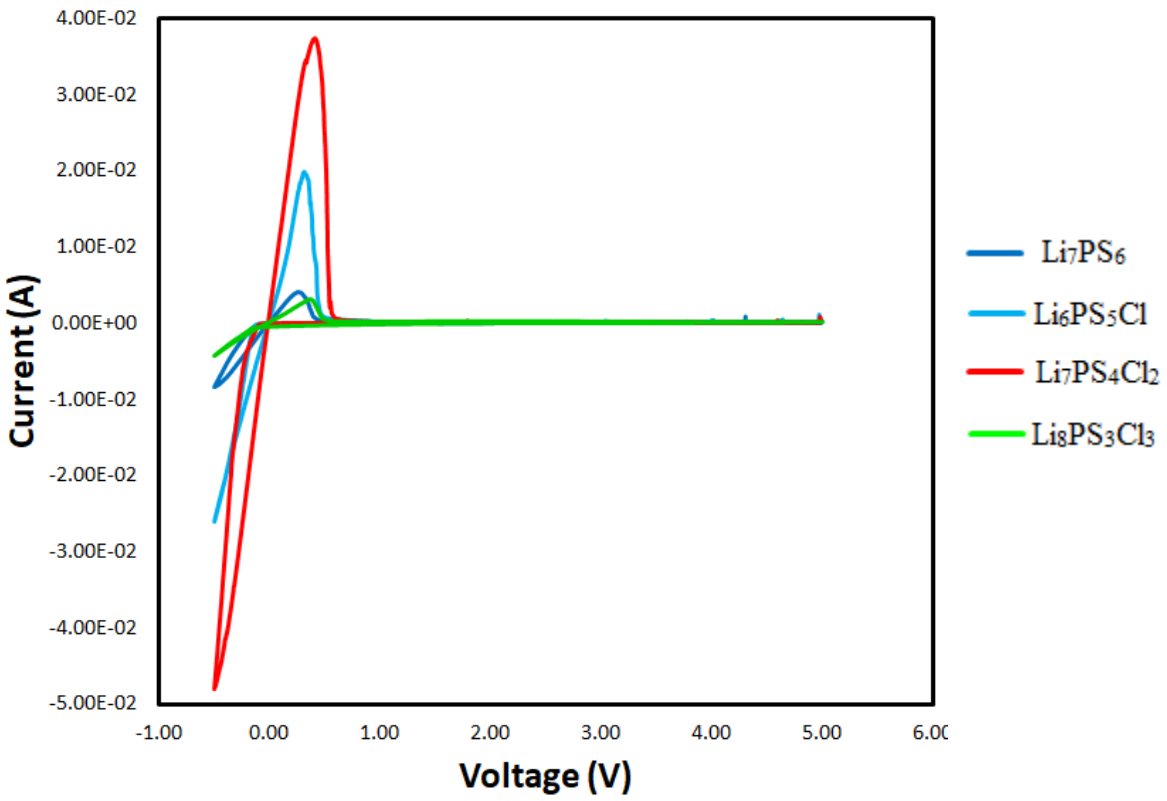

Figure 16. Results comparing different stoichiometric ratios of lithium argyrodite. The highest current is achieved in $Li_7PS_4Cl_2$

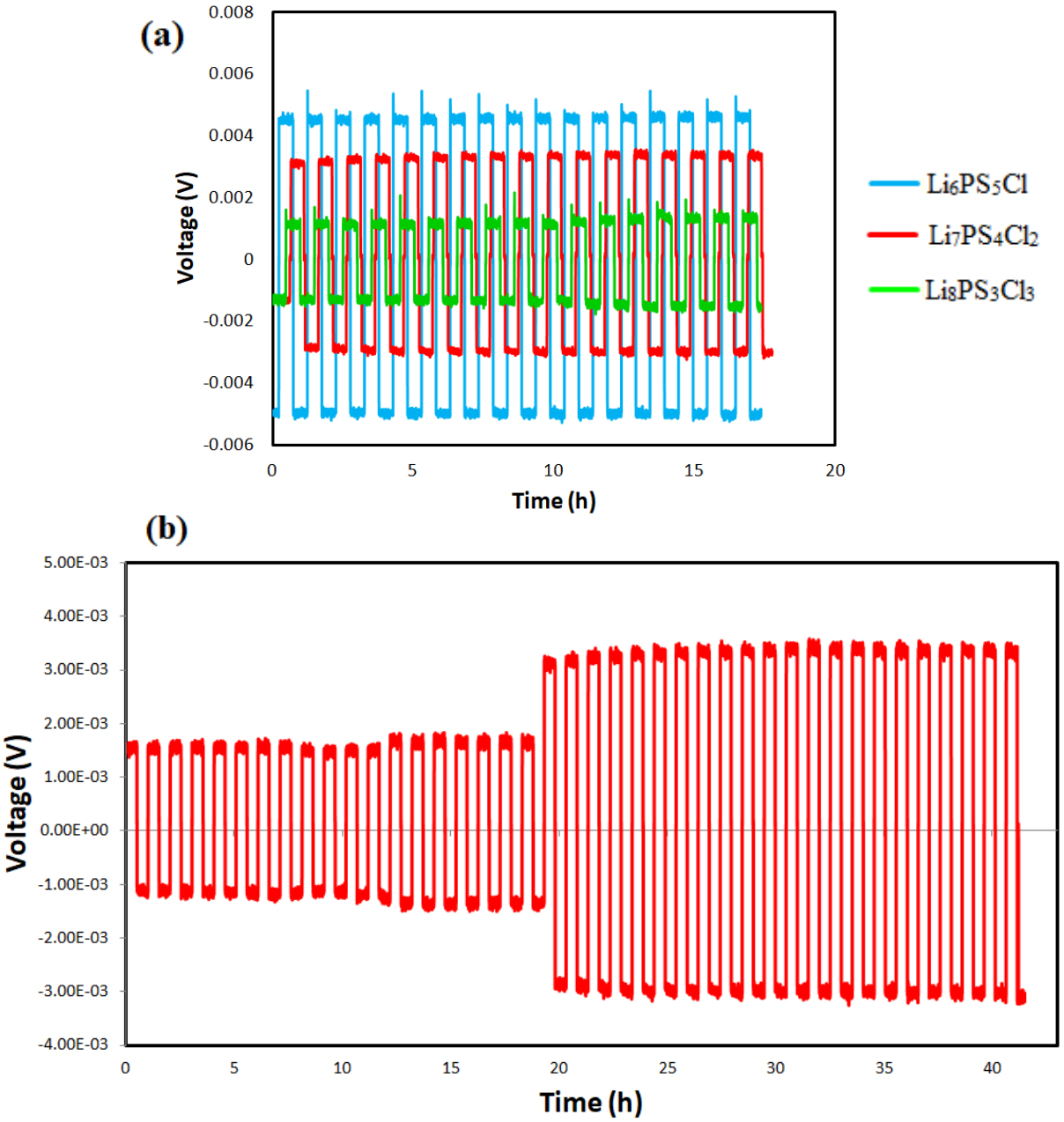

Figure 17. (a) Comparison of symmetric cell data of over 20 cycles at a current density of 0.02 mA cm^{-2}. (b) $Li_7PS_4Cl_2$ cycled first at 0.03 mA cm^{-2}- and then 0.05 mA cm^{-2}. The material stays stable over many cycles and a long period of time, indicating a fully formed electrode/electrolyte interface.

3.3 ANALYSIS OF PARAMETER-CONTROLLED LITHIUM ARGYRODITES

XRD was performed on all the process parameter-controlled controlled samples and grain size was estimated via the Scherrer Equation. All samples show XRD patterns in agreement with Li_6PS_5Cl (*figure 21*). The data supports a negative result, and indicates that mixing time and mechanical agitation do not have a pronounced effect on the grain size in Li_6PS_5Cl prepared via a liquid synthesis (*figure 22*). Further, these results indicate that grain size itself may have only a limited effect on the conductivity (within a range of 300-400 nm). Most previous work has indicated that the positive influence of larger grain size is seen when the crystallite reaches >400 nm [Bi, 2017]. This grain size was not able to be reliably produced via the experiment's methods, so no conclusions can be drawn on the effect that larger grain size may have.

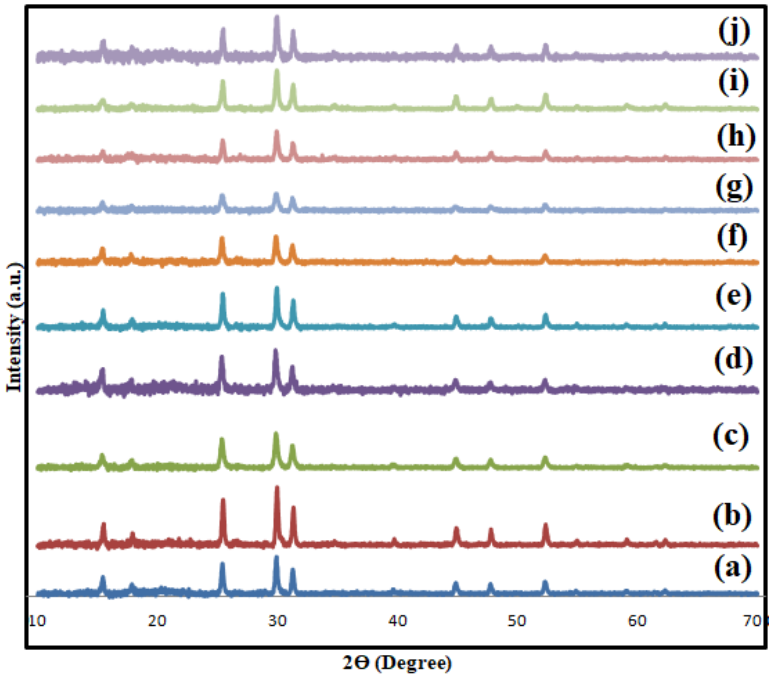

Figure 18. XRD patterns of the samples found in *Table 1*. No significant difference can be observed between the different samples. FWHM measurements from XRD were used in the calculation of crystallite size.

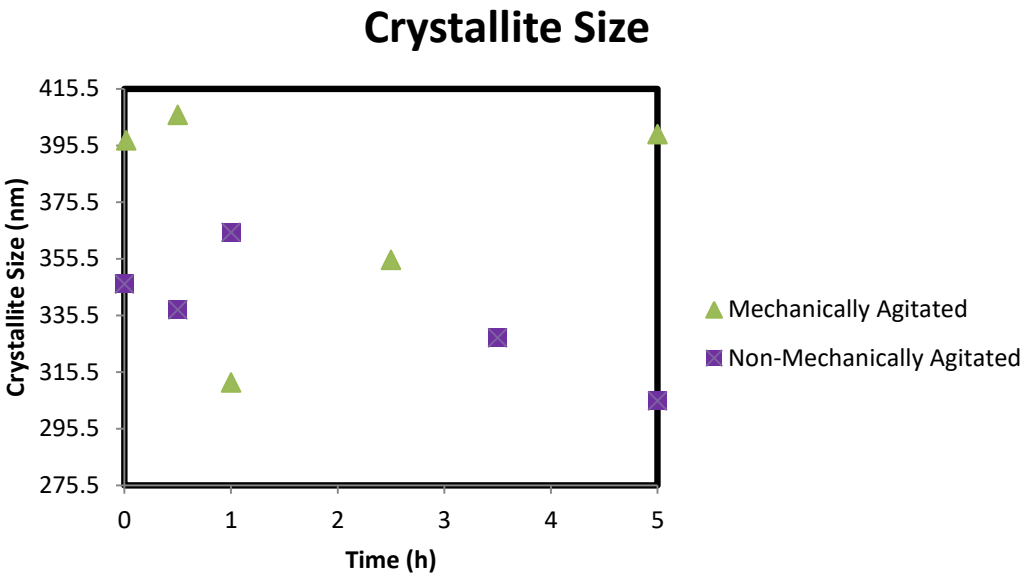

Figure 19. The crystallite size of mechanically and non-mechanically agitated verse mixing time. Grain size was not able to be significantly controlled for via this experiment's methods.

That said, there does appear to be a correlation between total mixing time and conductivity. For both the mechanically agitated and non-mechanically agitated samples, conductivity first increased with mixing time up to 1 hour. Following this, there appears to be a decrease in conductivity at 2.5–3 hours, before a sharp increase for groups when mixed for 5 hours. There is an overall positive trend line for both (*figure 24; figure 26*), and the maximum conductivity for both is roughly the same, indicating that total dissolution time is most important in this synthesis, and that the presence of mechanical agitation does not have a great effect. Ultimately, grain size was unable to be controlled

for via the given methods and no conclusive assessment can be made about its impact on the electrochemical performance of the solid electrolyte.

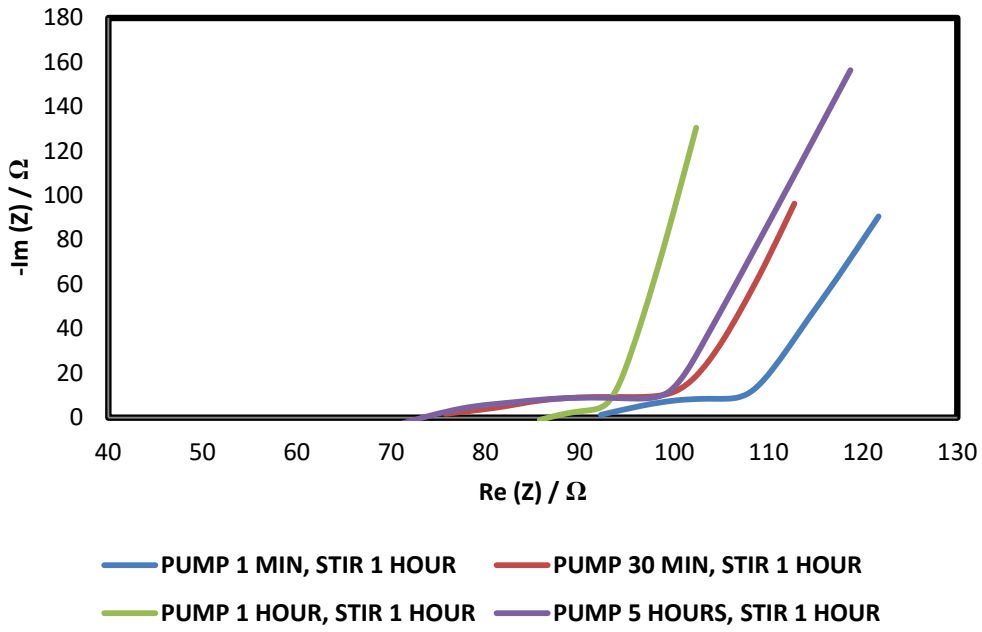

Figure 20. Nyquist plots of EIS data for 4 different pump-controlled mechanically agitated samples. Slower incorporation times correspond to less resistive solid electrolyte material.

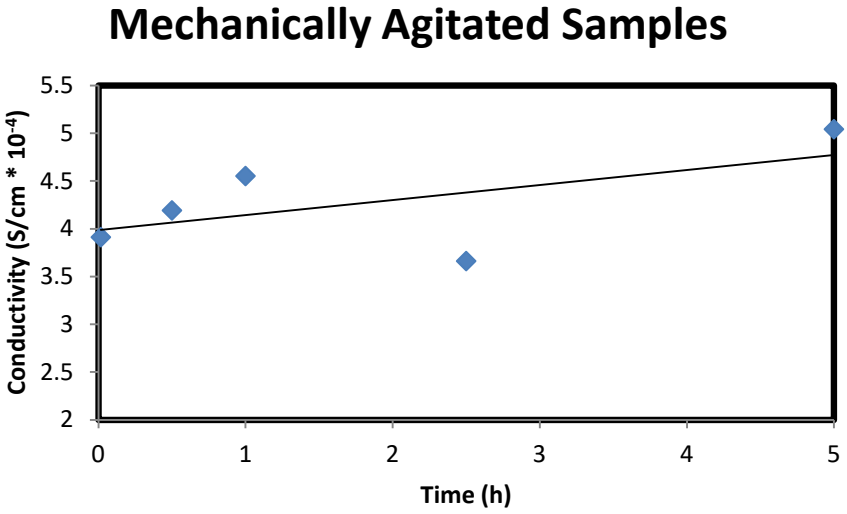

Figure 21. Mechanically agitated sample's conductivity verse time. When stirred for 5 hours, a maximum conductivity greater than $5 \times 10^{-4}\ S\ cm^{-1}$ is achieved.

The crystallite size of the mechanically agitated samples showed no trend over different mixing times, and all samples fell between 300 and 400 nm. There is, however, a positive trend that can be observed in the conductivity as mixing time increases (*figure 24*). All the mechanically agitated samples had a base stirring time of one hour, which was applied after pumping had finished. When the solution is pumped in and mixed very quickly (1 minute), the conductivity drops below 4×10^{-4} S cm^{-1}. Curiously, the conductivity drops lower when mixing time is 2.5 hours. Continuing to increase mixing time up to 5 hours yields a solid electrolyte with a conductivity over 5×10^{-4} S cm^{-1}.

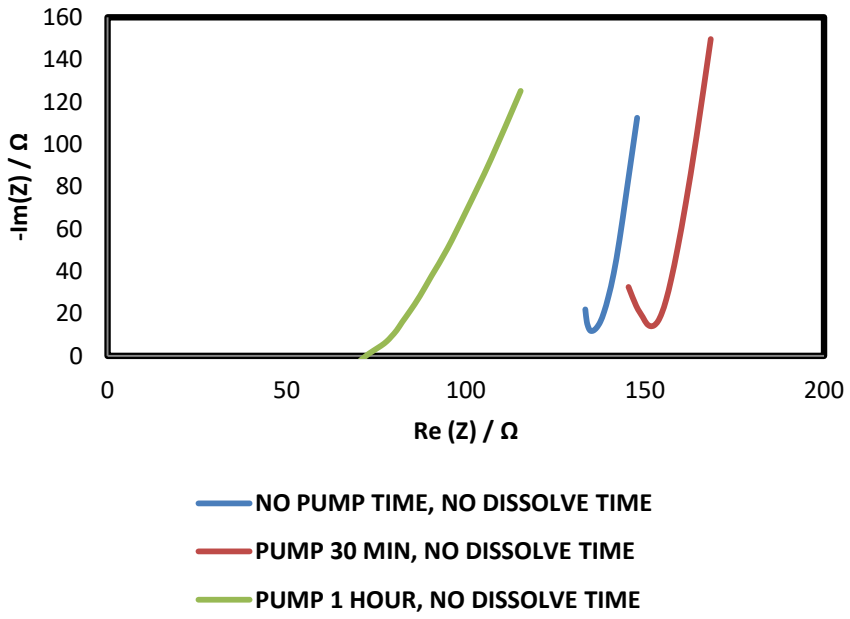

.

Figure 22. Nyquist plots of EIS data for 3 different pump-controlled, non-mechanically agitated samples. Mechanical agitation is not necessary for good performance, but a minimum of 1 hour dissolution time is required to synthesize a low resistance material.

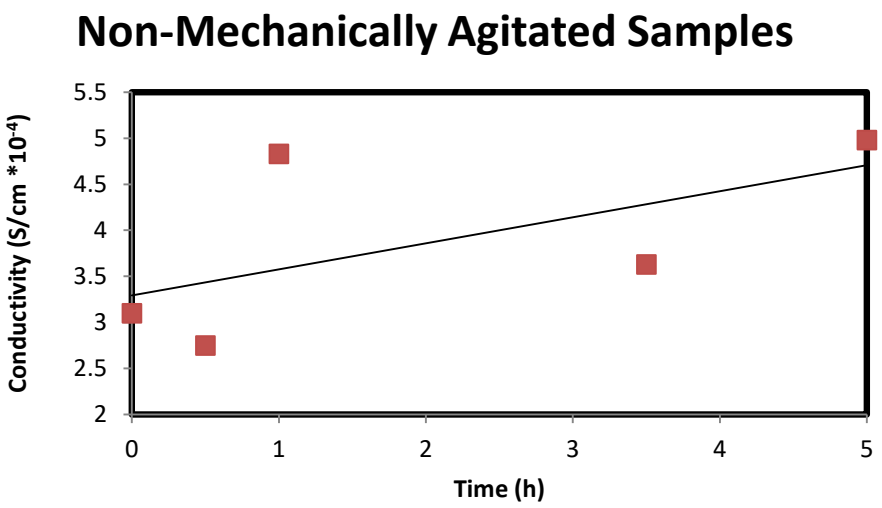

Figure 23. Non-mechanically agitated sample's conductivity verse time. When stirred for 5 hours, a maximum conductivity greater than 5×10^{-4} S $cm^{-1.}$

Unlike the stirred samples, the non-mechanically agitated samples did not have a baseline mixing time of 1 hour. Therefore the effects of no mixing time can be observed. When a sample is prepared by simply mixing the materials before immediately applying a heat treatment, this sample has amongst the worst conductivities of the group: around 3×10^{-4} S cm^{-1}. Only allowing for 30 minutes for mixing also gives poor results, yielding a solid electrolyte with an ionic conductivity of 2.75×10^{-4} S cm^{-1}. Interpreting these results in addition to the results from the mechanically agitated samples indicates that this synthesis needs at least an hour of synthesis time in order to achieve a good conductivity of 4×10^{-4} S cm^{-1}. Interestingly, there is also a dip in conductivity when the materials are mixed for 3.5 hours, a trend that was seen with the stirred samples. The best performance, however, was observed when the sample was prepared with 5 hours of mixing time. The conductivity for this sample was roughly the same as the mechanically agitated sample which underwent the same synthesis time. This indicates that total time

has a more pronounced effect on ionic conductivity than whether or not the solution is subject to stirring.

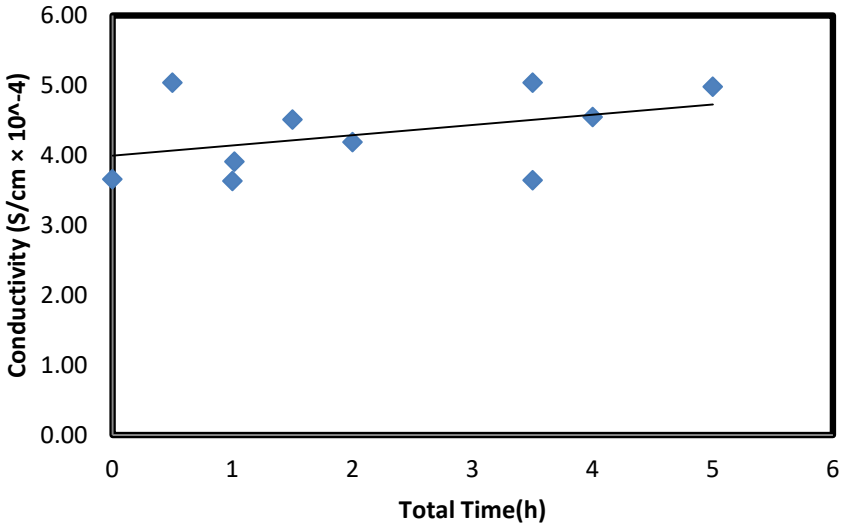

Figure 24. A scatter plot for all grain-controlled Li_6PS_5Cl samples of ionic conductivity verse mixing time, independent of mechanical agitation. There is a weak positive trend associating longer mixing times with higher conductivities.

When mechanical agitation is removed as a variable, a weak yet clear trend can be observed with respect to time. The two worst conductivities happen when there is less than 30 minutes of mixing time, while the best happen at either 1 hour or 5 hours of mixing time. However, it should be noted that all of these conductivities are relatively high when compared to many other solid electrolytes. Lithium argyrodites have been reported to have conductivities on the scale of 1×10^{-3} S cm^{-1}, but these are extremely energy and time intensive to produce. While grain size was ultimately not able to be controlled for, these results indicate that it is possible to synthesize Li_6PS_5Cl solid

electrolytes with good ionic conductivity by simply combining the requisite materials in ethanol and sintering at 200°C for 1 hour.

Another variable which is often controlled for to increase grain size is temperature. Generally speaking, a higher temperature will yield larger crystal size during sintering, and this seems to hold true for most solid electrolyte materials[Sharrafi, 2017; Bi, 2017; Ivanov, 2010]. For lithium argyrodites as well, researchers will often sinter as high as 550°C in order to synthesize their materials, and electrochemical performance often improves with increasing temperature [Boulineau, 2012]. Interestingly enough, this does not appear to be the case for our synthesized argyrodites. Using the standard synthesis techniques as described for preparing Li_6PS_5Cl—when the material is heated to 250°C for 1 hour as opposed to 200°C, the conductivity drops by a degree of magnitude to 10^{-5} S cm^{-1}.

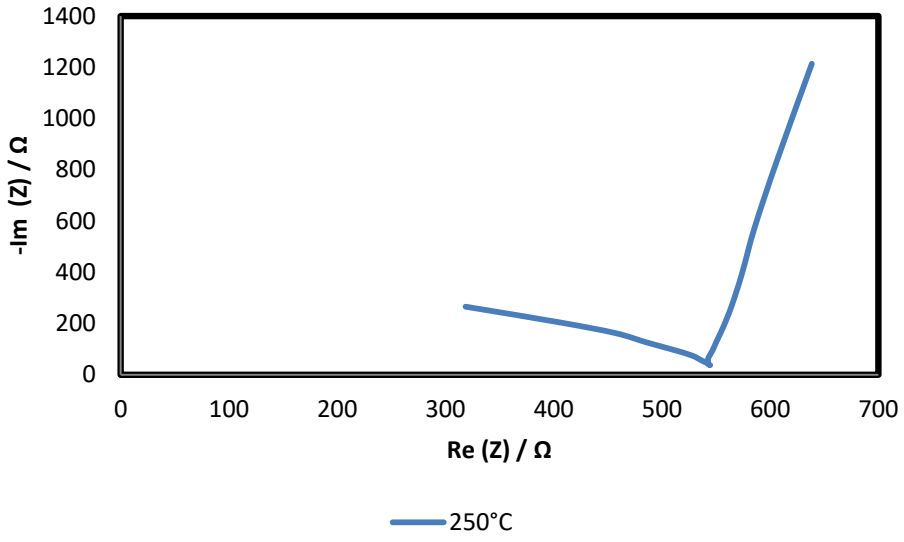

Figure 25. Nyquist plot of a Li_6PS_5Cl sample which has been annealed at 250°C. Its impedance is over 5 times that of samples annealed at 200°C.

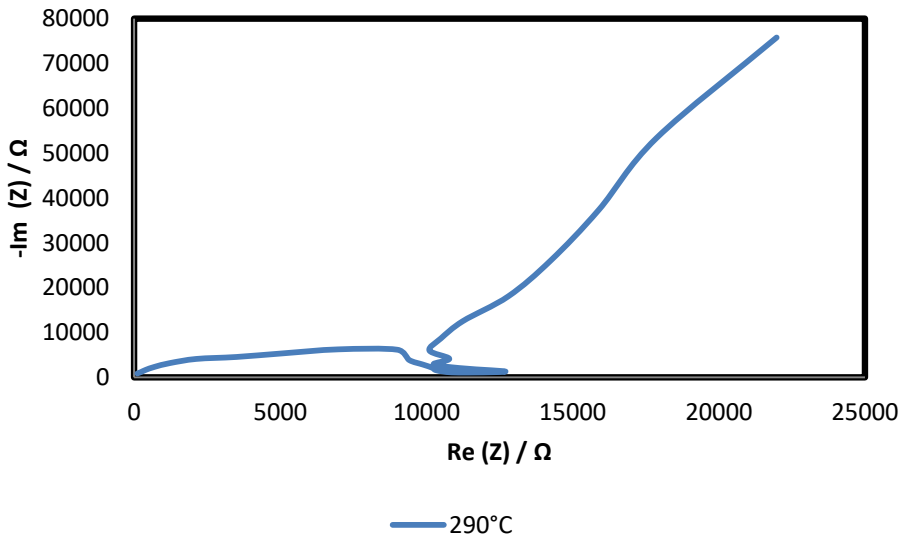

Figure 26. Nyquist plot of a Li6PS5Cl sample which has been annealed at 290°C. Its impedance is over 10 times that of samples annealed at 200°C.

When the temperature is pushed even higher to 290°C for 1 hour, the performance gets remarkably worse, and drops to a conductivity on the order of 10^{-6} S cm^{-1}. This can possibly be attributed to two things. First, our wet synthesis method introduces a solvent which is not a part of most synthesis procedures. By first mixing the materials in a solvent, the material is able to be produced much more efficiently than other methods, and in much shorter time. However it is possible that the presence of this solvent in trace amounts affects the chemical reactions which take place at higher temperature. Additionally, it is possible that issues arise due to the fact that sintering occurred under a vacuum. Other methods heat the materials in a sealed container, ensuring all the mass stays within. Under a vacuum and high heat, however, it is possible that sulfide ions become free and are sucked away, affecting

the chemical composition if pushed past a certain temperature. It appears that temperature is roughly 200°C, as anything past this (250 or 290°C) results in markedly worse performance.

4.0 CONCLUSIONS

Six stoichiometric combinations of Cl-doped lithium argyrodites were prepared and tested on their ionic conductivity, morphology, and electrochemical stability. The XRD patterns indicate a phase purity in all samples matching that of Li_6PS_5Cl. Addition of excess LiCl ($x \geq 2$) results in pure LiCl being present in the crystal structure, which likely contributes to the poor performance of these higher order molecules. Raman spectra was also captured, and a strong peak was observable at 421 cm^{-1}, which is attributable to the symmetric stretching mode of the P-S bond in PS_4^{3-}tetrahedra. The addition of excess LiCl does not appear to affect the vibrational modes of the samples.

Concerning ionic conductivity, the pure argyrodite Li_7PS_6 performs poorly, achieving a conductivity of only 1.9×10^{-5} S cm^{-1}. Through halide doping, LiCl is added to the molecular structure, which improves the conductivity ten-fold to a value of 2×10^{-4} S cm^{-1}. The addition of LiCl continues to benefit the electrolyte's perfomance, achieving its maximum value of 4.5×10^{-4} S cm^{-1} with a stoichiometric structure of $Li_7PS_4Cl_2$. This trend continues with regards to activation energy, as $Li_7PS_4Cl_2$ had the lowest of all the tested samples, at 0.25 eV. Both of these values are excellent for lithium argyrodite solid electrolytes in general, and are the best yet reported for argyrodites prepared via the novel, fast and inexpensive liquid synthesis method. All materials showed short-term stability up to 5V, indicating a positive reaction with a metal lithium

electrode. All the materials also showed great long-term stability when applied to current densities of 0.02–0.05 mA cm^{-2}.

Samples were also prepared with the intention of controlling for grain size via the different common methods: control of mixing time, control of sintering temperature, and control of mechanical agitation. Ultimately, no method tested was able to reliably achieve crystal sizes significantly greater than 400 nm, the size at which other sulfide-based electrolyte materials have been reported to achieve enhanced performance. As such, no conclusive statement can be made with regards to grain size and ionic conductivity for lithium argyrodites. There does appear to be a correlation between synthesis time and conductivity, however, with a minimum of 1 hour needed to produce good results. A longer synthesis time of 5 hours is even more beneficial, yielding a solid electrolyte with a conductivity of over 5×10^{-4} S cm^{-1}.

This work reveals the ease and inexpensive reliability with which suitable solid electrolytes can be synthesized in just three hours, potentially opening possibilities for commercial use. Additionally, this thesis gives invaluable insight and furthers understanding of the synthesis of lithium argyrodites through liquid synthesis methods, which will factor in to future of all-solid-state battery technology.

REFERENCES

Auvergniot, J., Cassel, A., Foix, D., Viallet, V., Seznec, V., and Dedryvère, R. (2017a). Redox activity of argyrodite Li6PS5Cl electrolyte in all-solid-state Li-ion battery: An XPS study. Solid State Ionics *300*, 78–85.

Auvergniot et al. (2017b). Interface Stability of Argyrodite Li6PS5Cl toward LiCoO2, LiNi1/3Co1/3Mn1/3O2, and LiMn2O4 in Bulk All-Solid-State Batteries - Chemistry of Materials (ACS Publications).

Bachman, J.C., Muy, S., Grimaud, A., Chang, H.-H., Pour, N., Lux, S.F., Paschos, O., Maglia, F., Lupart, S., Lamp, P., et al. (2016). Inorganic Solid-State Electrolytes for Lithium Batteries: Mechanisms and Properties Governing Ion Conduction. Chem. Rev. *116*, 140–162.

Bi, H., Liu, X., Zhu, L., Sun, J., Yu, S., Yu, H., and Pei, L. (2017). Effect of MgO addition and grain size on the electrical properties of Ce0.9Gd0.1O1.95 electrolyte for IT-SOFCs. International Journal of Hydrogen Energy *42*, 11735–11744.

Boulineau, S., Courty, M., Tarascon, J.-M., and Viallet, V. (2012). Mechanochemical synthesis of Li-argyrodite Li6PS5X (X=Cl, Br, I) as sulfur-based solid electrolytes for all solid state batteries application. Solid State Ionics *221*, 1–5.

Boulineau, S., Tarascon, J.-M., Leriche, J.-B., and Viallet, V. (2013). Electrochemical properties of all-solid-state lithium secondary batteries using Li-argyrodite Li6PS5Cl as solid electrolyte. Solid State Ionics *242*, 45–48.

Chen, M., and Adams, S. (2015). High performance all-solid-state lithium/sulfur batteries using lithium argyrodite electrolyte. J Solid State Electrochem *19*, 697–702.

Chen, H.M., Maohua, C., and Adams, S. (2015). Stability and ionic mobility in argyrodite-related lithium-ion solid electrolytes. Phys. Chem. Chem. Phys. *17*, 16494–16506.

Chen, M., Prasada Rao, R., and Adams, S. (2014). The unusual role of Li6PS5Br in all-solid-state CuS/Li6PS5Br/In–Li batteries. Solid State Ionics *268*, 300–304.

Chida, S., Miura, A., Rosero-Navarro, N.C., Higuchi, M., Phuc, N.H.H., Muto, H., Matsuda, A., and Tadanaga, K. (2018). Liquid-phase synthesis of Li6PS5Br using ultrasonication and application to cathode composite electrodes in all-solid-state batteries. Ceramics International *44*, 742–746.

Dawson, J.A., Canepa, P., Famprikis, T., Masquelier, C., and Islam, M.S. (2018). Atomic-Scale Influence of Grain Boundaries on Li-Ion Conduction in Solid Electrolytes for All-Solid-State Batteries. J. Am. Chem. Soc. *140*, 362–368.

Deiseroth, H.-J., Kong, S.-T., Eckert, H., Vannahme, J., Reiner, C., Zaiß, T., and Schlosser, M. (2008). Li6PS5X: A Class of Crystalline Li-Rich Solids With an Unusually High Li+ Mobility. Angewandte Chemie International Edition *47*, 755–758.

Deiseroth, H.-J., Maier, J., Weichert, K., Nickel, V., Kong, S.-T., and Reiner, C. (2011). Li7PS6 and Li6PS5X (X: Cl, Br, I): Possible Three-dimensional Diffusion Pathways for Lithium Ions and Temperature Dependence of the Ionic Conductivity by Impedance Measurements. Z. Anorg. Allg. Chem. *637*, 1287–1294.

Han, F., Yue, J., Fan, X., Gao, T., Luo, C., Ma, Z., Suo, L., and Wang, C. (2016). High-Performance All-Solid-State Lithium–Sulfur Battery Enabled by a Mixed-Conductive Li2S Nanocomposite. Nano Lett. *16*, 4521–4527.

Huber, T.M., Navickas, E., Sasaki, K., Yildiz, B., Hutter, H., Tuller, H., and Fleig, J. (2018). Interplay of Grain Size Dependent Electronic and Ionic Conductivity in Electrochemical Polarization Studies on Sr-Doped LaMnO3 (LSM) Thin Film Cathodes. J. Electrochem. Soc. *165*, F702–F709.

Huo, D., Baldinozzi, G., Siméone, D., Khodja, H., and Surblé, S. (2016). Grain size-dependent electrical properties of La1.95Sr0.05Zr2O7-δ as potential Proton Ceramic Fuel Cell electrolyte. Solid State Ionics *298*, 35–43.

Ivanov, V.V., Shkerin, S.N., Rempel, A.A., Khrustov, V.R., Lipilin, A.S., and Nikonov, A.V. (2010). Electrical conductivity of zirconia-based solid electrolyte with submicron grain size. Dokl Phys Chem *433*, 125–127.

Kim, D.H., Oh, D.Y., Park, K.H., Choi, Y.E., Nam, Y.J., Lee, H.A., Lee, S.-M., and Jung, Y.S. (2017). Infiltration of Solution-Processable Solid Electrolytes into Conventional Li-Ion-Battery Electrodes for All-Solid-State Li-Ion Batteries. Nano Lett. *17*, 3013–3020.

Kraft, M.A., Culver, S.P., Calderon, M., Böcher, F., Krauskopf, T., Senyshyn, A., Dietrich, C., Zevalkink, A., Janek, J., and Zeier, W.G. (2017). Influence of Lattice Polarizability on the Ionic Conductivity in the Lithium Superionic Argyrodites Li6PS5X (X = Cl, Br, I). J. Am. Chem. Soc. *139*, 10909–10918.

Liu, Z., Fu, W., Payzant, E.A., Yu, X., Wu, Z., Dudney, N.J., Kiggans, J., Hong, K., Rondinone, A.J., and Liang, C. (2013). Anomalous High Ionic Conductivity of Nanoporous β-Li3PS4. J. Am. Chem. Soc. *135*, 975–978.

Ma, Z., Xue, H.-G., and Guo, S.-P. (2018a). Recent achievements on sulfide-type solid electrolytes: crystal structures and electrochemical performance. J Mater Sci *53*, 3927–3938.

McKissock, B., Loyselle, P., and Vogel, E. Guidelines on Lithium-ion Battery Use in Space Applications. 54.

Phuc, N.H.H., Morikawa, K., Mitsuhiro, T., Muto, H., and Matsuda, A. (2017). Synthesis of plate-like Li<Subscript>3</Subscript>PS<Subscript>4</Subscript> solid electrolyte via liquid-phase shaking for all-solid-state lithium batteries. Ionics *23*, 2061–2067.

Rao, R.P., and Adams, S. (2011). Studies of lithium argyrodite solid electrolytes for all-solid-state batteries. Phys. Status Solidi A *208*, 1804–1807.

Rao, R.P., Sharma, N., Peterson, V.K., and Adams, S. (2013). Formation and conductivity studies of lithium argyrodite solid electrolytes using in-situ neutron diffraction. Solid State Ionics *230*, 72–76.

Rayavarpu (2011). Variation in structure and Li+-ion migration in argyrodite-type Li6PS5X (X = Cl, Br, I) solid electrolytes | SpringerLink.

Sharafi, A., Haslam, C.G., Kerns, R.D., Wolfenstine, J., and Sakamoto, J. (2017). Controlling and correlating the effect of grain size with the mechanical and electrochemical properties of Li7La3Zr2O12 solid-state electrolyte. J. Mater. Chem. A *5*, 21491–21504.

Walker, W., Yayathi, S., Shaw, J., and Ardebili, H. (2015). Thermo-electrochemical evaluation of lithium-ion batteries for space applications. Journal of Power Sources *298*, 217–227.

Wang, H., Hood, Z.D., Xia, Y., and Liang, C. (2016). Fabrication of ultrathin solid electrolyte membranes of β-Li3PS4 nanoflakes by evaporation-induced self-assembly for all-solid-state batteries. J. Mater. Chem. A *4*, 8091–8096.

Wang, Y., Richards, W.D., Ong, S.P., Miara, L.J., Kim, J.C., Mo, Y., and Ceder, G. (2015). Design principles for solid-state lithium superionic conductors. Nature Materials *14*, 1026–1031.

Wang, Y., Lu, D., Bowden, M., El Khoury, P.Z., Han, K.S., Deng, Z.D., Xiao, J., Zhang, J.-G., and Liu, J. (2018). Mechanism of Formation of Li $_7$ P $_3$ S $_{11}$ Solid Electrolytes through Liquid Phase Synthesis. Chemistry of Materials *30*, 990–997.

Wu, J.-F., and Guo, X. (2017). Origin of the low grain boundary conductivity in lithium ion conducting perovskites: Li3xLa0.67−xTiO3. Phys. Chem. Chem. Phys. *19*, 5880–5887.

Yu, C., Ganapathy, S., de Klerk, N.J.J., Roslon, I., van Eck, E.R.H., Kentgens, A.P.M., and Wagemaker, M. (2016a). Unravelling Li-Ion Transport from Picoseconds to Seconds: Bulk versus Interfaces in an Argyrodite Li6PS5Cl–Li2S All-Solid-State Li-Ion Battery. J. Am. Chem. Soc. *138*, 11192–11201.

Yu, C., van Eijck, L., Ganapathy, S., and Wagemaker, M. (2016b). Synthesis, structure and electrochemical performance of the argyrodite Li6PS5Cl solid electrolyte for Li-ion solid state batteries. Electrochimica Acta *215*, 93–99.

Yubuchi, S., Teragawa, S., Aso, K., Tadanaga, K., Hayashi, A., and Tatsumisago, M. (2015). Preparation of high lithium-ion conducting Li6PS5Cl solid electrolyte from ethanol solution for all-solid-state lithium batteries. Journal of Power Sources *293*, 941–945.

Zhang, Z., Zhang, L., Liu, Y., Yu, C., Yan, X., Xu, B., and Wang, L. (2018). Synthesis and characterization of argyrodite solid electrolytes for all-solid-state Li-ion batteries. Journal of Alloys and Compounds *747*, 227–235.

Ziolkowska, D., Arnold, W., Druffel, T., Sunkara, M., Wang, H. (2018) Rapid and economic synthesis of Li_7PS_6 Solid Electrolyte from Liquid Approach. Submitted.

CURRICULUM VITA

NAME: William Richard Arnold

ADDRESS: J.B. SPEED SCHOOL OF ENGINEERING
University of Louisville
132Eastern Pkwy.
Louisville, Kentucky 40292

DOB: Louisville, Kentucky - September 27, 1993

EDUCATION
& TRAINING: B.S. Biosystems Engineering
University of Kentucky
2012-2016

M.S. Mechanical Engineering
University of Louisville
2017-2018